



HAL
open science

African/Amazonian Proterozoic correlations of Iberia: A detrital zircon U-Pb study of early Cambrian conglomerates from the Sierra de la Demanda (northern Spain)

B. Abalos, J.I. Gil Ibarguchi, M.E. Sánchez-Lorda, Jean-Louis Paquette

► To cite this version:

B. Abalos, J.I. Gil Ibarguchi, M.E. Sánchez-Lorda, Jean-Louis Paquette. African/Amazonian Proterozoic correlations of Iberia: A detrital zircon U-Pb study of early Cambrian conglomerates from the Sierra de la Demanda (northern Spain). *Tectonics*, 2012, 31, pp.TC3003. 10.1029/2011TC003041. hal-00696146

HAL Id: hal-00696146

<https://hal.science/hal-00696146>

Submitted on 29 Nov 2021

HAL is a multi-disciplinary open access archive for the deposit and dissemination of scientific research documents, whether they are published or not. The documents may come from teaching and research institutions in France or abroad, or from public or private research centers.

L'archive ouverte pluridisciplinaire **HAL**, est destinée au dépôt et à la diffusion de documents scientifiques de niveau recherche, publiés ou non, émanant des établissements d'enseignement et de recherche français ou étrangers, des laboratoires publics ou privés.

Copyright

African/Amazonian Proterozoic correlations of Iberia: A detrital zircon U-Pb study of early Cambrian conglomerates from the Sierra de la Demanda (northern Spain)

B. Ábalos,¹ J. I. Gil Iburguchi,² M. E. Sánchez-Lorda,^{1,3} and J. L. Paquette⁴

Received 7 October 2011; revised 8 March 2012; accepted 20 March 2012; published 8 May 2012.

[1] Unfoliated conglomerates define the base of an Early Cambrian transgressive system tract in the Sierra de la Demanda. Correlations allow us to bracket the corresponding sechron between 532 Ma and 520–521 Ma. These conglomerates contain sandstone and metamorphic quartzite pebbles carrying detrital tourmaline, rutile and zircon grains of plutonic or medium- to high-grade metamorphic derivation. Zircon detrital grains exhibit concordant or sub-concordant U/Pb ages clustered in various groups, including Neoproterozoic (2.52–2.56 Ga), Paleoproterozoic (1.71–2.02 Ga), and Mesoproterozoic (1.47 and ca. 1.1–1.0 Ga), the latter representative of orogenic magmatism related to Rodinia supercontinental assembly. The Neoproterozoic is represented by concordant ages in the range 750–880 Ma and by Cryogenian discordant ages. Ediacaran zircons cluster in two subsets ranging between 590 and 680 Ma and 560–585 Ma, both including several concordant ages. They reflect formation of juvenile crust in magmatic arc and back-arc basin settings. Zircon ages younger than 520–525 Ma postdate the depositional age of the conglomerate and may represent Hercynian overprinting. Bibliographic data overlooked in other provenance studies indicate that Mesoproterozoic relics as those presented here should no longer be considered of exotic origin with respect to a Gondwanan (West African) affinity of the Neoproterozoic to early Paleozoic of Iberia. The proposed source area, the “Ebro Massif” of central-north Iberia, currently is concealed under a kilometer-thick Paleozoic or younger cover. Its tectonic organization would compare to that of the North African or Amazonian cratons (including Mesoproterozoic components), rather than to the Neoproterozoic arc settings described in northwest and southwest Iberia.

Citation: Ábalos, B., J. I. Gil Iburguchi, M. E. Sánchez-Lorda, and J. L. Paquette (2012), African/Amazonian Proterozoic correlations of Iberia: A detrital zircon U-Pb study of early Cambrian conglomerates from the Sierra de la Demanda (northern Spain), *Tectonics*, 31, TC3003, doi:10.1029/2011TC003041.

1. Introduction

[2] Resolving tectonic problems by dating detrital minerals has received increasing attention during the last decade, notably helped by the increased use of laser ablation-inductively coupled plasma-mass spectrometry (LA-ICP-MS) in U/Pb

geochronology. This method has become a widely used approach for the study of sediment provenance, timing of tectonic processes, mountain building cycles, dating of multiple tectono-metamorphic or tectono-magmatic events encapsulated in a single mineral grain (most often zircon), establishment of otherwise undatable or difficult to resolve maximum depositional ages of sedimentary units, source-sedimentary basin evolution, and for the reconstruction of paleocontinental masses [Condie and Aster, 2009; Carrapa, 2010]. The method has shown some weaknesses (failure to record some tectonic events [e.g., Hietpas et al., 2010]) or biases [Andersen, 2005; Lawrence et al., 2010], but is generally robust.

[3] Detrital zircons may be derived from sources removed by erosion, currently buried in the subsurface, or missed. It is assumed that the age distribution in a detrital zircon population represents the bulk age distribution of the continental crust sampled, although some local sources may dominate over others. Similarly, such populations permit to identify

¹Departamento de Geodinámica, Universidad del País Vasco UPV/EHU, Bilbao, Spain.

²Departamento de Mineralogía y Petrología, Universidad del País Vasco UPV/EHU, Bilbao, Spain.

³Servicio General de Geocronología y Geoquímica Isotópica-SGiker IBERCRON, Universidad del País Vasco UPV/EHU, Bilbao, Spain.

⁴Equipe de Géochimie, Laboratoire Magmas et Volcans, UMR 6524, CNRS, Université B. Pascal, Clermont-Ferrand, France.

Corresponding author: B. Ábalos, Departamento de Geodinámica, Universidad del País Vasco UPV/EHU, PO Box 644, E-48080 Bilbao, Spain. (benito.abalos@ehu.es)

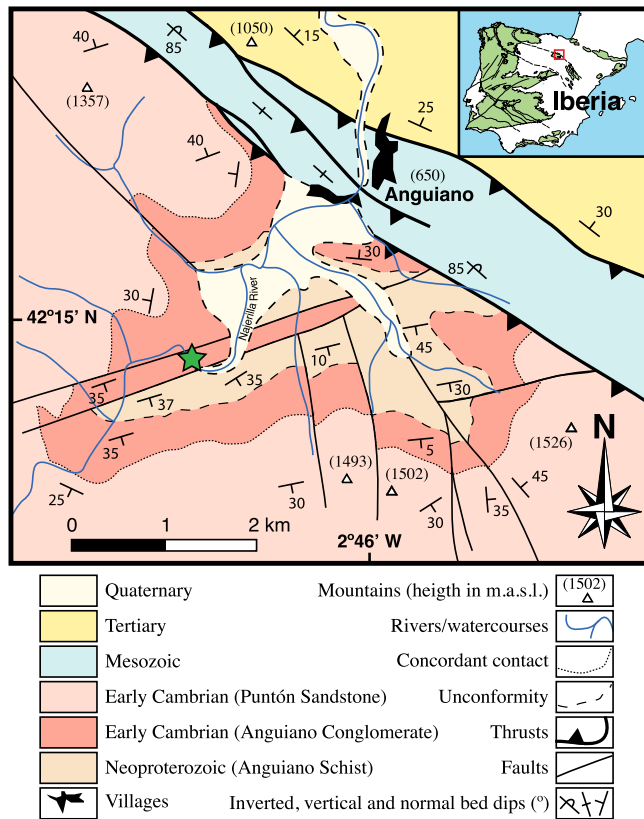


Figure 1. Geological sketch map [after *Ramírez-Merino et al.*, 1990] of the area to the South of Anguiano and (inset) regional geological context of the Sierra de la Demanda massif in the Iberian Peninsula. Green domains in inset indicate pre-Alpine basement. Sampling site (star) coordinates are: latitude $42^{\circ}15'6.37''\text{N}$, longitude $2^{\circ}46'47.95''\text{W}$, also UTM 30, X518149, Y4677754.

and correlate cratons and orogens of any age (or portions of them) preserved in current continents [*Condie et al.*, 2011].

[4] The Cambrian of the Iberian Peninsula has traditionally been divided into a lower siliciclastic succession, a middle carbonate sequence and upper siliciclastic units. These rock series are thick (>2000 m), regionally diachronic and were deposited in shallow marine environments under transgressive-regressive cycles. Though their base usually overlies older rocks unconformably, locally an apparently conformable lithostratigraphic contact separates upper, coarser siliciclastics from underlying finer ones. The latter are commonly Neoproterozoic, though locally they can contain earliest Cambrian trace fossils, acritarchs or trilobites (see *Liñán et al.* [2002] for further details). The oldest rocks of the lower siliciclastic succession are always early Cambrian conglomerates and sandstones and their basal contact brackets a hiatus of variable duration around the Ediacaran-Cambrian boundary [*Liñán et al.*, 2002]. These rocks contain relics of a currently concealed pre-Cambrian and pre-Ediacaran basement whose study can shed light on its organization. In this context, we present the results of a geochronological study that can be devised to identify the provenance of detrital zircon grains and, with complementary microtectonic, petrofabric and geochemical evidences,

the source region of igneous, metamorphic and sedimentary conglomerate pebbles.

2. Geological Context

[5] The “Sierra de la Demanda” is a pre-Mesozoic massif located at the northwestern extension of the Iberian Ranges (Figure 1). It contains thick Cambro-Ordovician successions sedimentologically similar to coeval series of the central Iberian Ranges and the West-Asturian-Leonese Zone of the Iberian Massif [*Liñán et al.*, 2002]. Unmetamorphosed Triassic siliciclastics (Germano-type “Buntsandstein” facies) and younger successions rest unconformably on Paleozoic rocks mildly metamorphosed and deformed during the Carboniferous [*Colchen*, 1974]. Alpine tectonic inversion reworked both Paleozoic and younger rocks during the Cenozoic [*Capote et al.*, 2002].

2.1. The Neoproterozoic of the Sierra de la Demanda

[6] Precambrian successions of the Sierra de la Demanda relate to the Neoproterozoic era and compare to those of the Iberian Peninsula at a wider scale. They often occur under unconformable Paleozoic sediments [*Vidal et al.*, 1994] and both the paleontological discoveries and the radiometric datings performed so far yielded in most cases Ediacaran (i.e., ranging between 635 and 542 ± 1 Ma) depositional ages [*Valladares et al.*, 2002a, 2002b; *Liñán et al.*, 2002]. These rocks were regionally deformed, locally intruded by igneous suites, and mildly metamorphosed before the Cambrian in most parts of the Iberian Massif. This was also the case in the Sierra de la Demanda and elsewhere in the Iberian Ranges [*Álvaro et al.*, 2008]. This tectonic activity permits to disclose a late Neoproterozoic to early Cambrian (Cadomian) orogeny in Iberia. It is widely acknowledged that a magmatic arc and a back-arc basin are the Cadomian tectonic settings preserved [e.g., *Ugidos et al.*, 1997; *Eguiluz et al.*, 2000].

[7] Neoproterozoic rocks in the Sierra de la Demanda are represented by azoic, dark siltstones and mudstones with interbedded sandstone layers. These rocks are currently tectonites (foliated slates with intersection lineations and crenulation microfolds) and are known as the “Anguiano Schists” [cf. *Colchen*, 1974] (Figures 1 and 2). Their maximum observable thickness is 100–150 m [*Ramírez-Merino et al.*, 1990]. The contact between Cambrian and pre-Cambrian successions is unconformable, the Neoproterozoic rocks bearing a more protracted and complex tectonic history than the overlying rocks [*Ábalos et al.*, 2011].

2.2. The Cambrian of the Sierra de la Demanda

[8] *Colchen* [1974] disclosed the stratigraphic, structural and map organization of Cambrian rocks resting upon azoic sediments in the “Sierra de la Demanda” (Figure 2), whereas *Shergold et al.* [1983] refined their stratigraphical organization and *Ramírez-Merino et al.* [1990] updated their map distribution. These successions comprise a number of lithostratigraphic units that can be categorized into two depositional sequences laid down during a time interval (called “sechron”) limited by the ages of their boundaries, which thus bear chronostratigraphic significance (Figure 2). The lower one is a transgressive system tract made of early Cambrian strata delimited by an angular unconformity at the base (likely a sequence boundary with erosional incision)

and a hiatus at the top (related to a maximum flooding surface). The upper sequence is a composite high-stand system tract that begins with likely condensed, paleontologically dated middle Cambrian marine beds [Liñán *et al.*, 1993, 2002]. It continues with thick shelf, shallow marine and transitional siliciclastics reaching the Lower Ordovician (Tremadocian).

[9] The largest outcrops of the lowermost, transgressive system tract occur in the northeastern part of the Sierra de la Demanda (Figure 1). These are azoic, predominantly siliciclastic rocks. A basal (up to 300 m thick) quartz-rich conglomeratic formation (“Anguiano Conglomerate”) is conformably overlain by an up to 500 m thick sandstone and quartzite formation (“Puntón sandstone”) that includes an upper silty to slaty segment (“Riocabado beds”), and then by a 50–150 m thick azoic dolomite (“Urbión dolomite”). This permits correlation with comparable lithostratigraphic successions of the Iberian Ranges and the Iberian Peninsula whose fossil content enabled its dating. As a result of this correlation, a lower Corduban to middle Marianian age has been assigned to the early Cambrian system tract of the Sierra de la Demanda [Liñán *et al.*, 2002].

3. Chronostratigraphy of the Early Cambrian Sechron

[10] Chronostratigraphical upper and lower age limits for the early Cambrian system tract of the Sierra de la Demanda (the early Cambrian sechron) is hampered by the fact that Cambrian chronostratigraphy is currently under discussion. The Cambrian period is marked by the appearance and rapid diversification (the “Cambrian explosion”) of metazoans with mineralized skeletons. Trilobites, archaeocyathans, acritarchs and inarticulate brachiopods provide biostratigraphically useful markers. However, global ones are scarce in the Early Cambrian. Provincialism has led to establishment of regional subdivisions of the Cambrian and no stage scheme suitable for regional use exists so far for this period. This contrasts with the case of the middle and late Cambrian, for which internationally acceptable stages have been established based upon global biostratigraphical markers [Shergold and Cooper, 2004; Peng and Babcock, 2008] (Figure 2). Iberian correlations with other regional stage subdivisions include those for which a comprehensive paleontological knowledge is available (notably from Morocco, Siberia and Laurentia), as well as some precise radiometric datings [e.g., Maloof *et al.*, 2010a, 2010b] (Figure 2). However, translation of regional correlations into radiometric ages is difficult currently.

[11] The subdivision of the Cambrian into series/epochs [Babcock and Peng, 2007] contrasts with the long-standing threefold subdivision of the Cambrian [Shergold and Cooper, 2004] into early (from 542 ± 1 to 513 ± 2 Ma), middle (from 513 ± 2 to 501 ± 2 Ma) and late (from 501 ± 2 to 488.31.7 Ma) series/epochs (Figure 2). The regional stage nomenclatures are based upon this threefold subdivision and both inter-regional paleontological correlations and most radiometric datings take it as a reference.

[12] Lower and Middle Cambrian regional stages defined for the Iberian Peninsula are the Corduban, Ovetian, Marianian and Bilbilian for the lower Cambrian and the Leonian,

Caesar-Augustan and Languedocian for the middle Cambrian [Liñán *et al.*, 1993, and references therein]. The Corduban stage contains ichnofossil assemblages correlatable with other sequences around the world, notably with the Nemakit-Daldynian and Tommotian regional stages of Siberia. The boundary between the Nemakit-Daldynian (older stage) and the Tommotian (younger stage) marks the first appearance of metazoan reefs and calcite biomineralizers (the first brachiopods and archaeocyatha) and new zircon ^{206}Pb - ^{238}U ages constrain its timing to 524.84 ± 0.09 Ma [Maloof *et al.*, 2010b]. Iberian Corduban beds contain bigotinid trilobites [Liñán *et al.*, 2005]. In the Siberian stages, however, the first trilobites are reported to occur later, at the base of the Atdabanian stage (which succeeds the Tommotian), presumably 518–519 Ma ago. Correlations based upon shared Siberian and Moroccan fossil assemblages together with radiometric dating of tuffs interbedded with the latter [Maloof *et al.*, 2010b] suggest that the Tommotian – Atdabanian limit is slightly younger than 520.93 ± 0.14 Ma. This follows closely the agreement of the International Commission on Stratigraphy, which establishes the first appearance of trilobites about 521 Ma ago, coinciding with the findings from Morocco, Russia, Spain and Laurentia [Babcock *et al.*, 2005]. In Siberia, thus, trilobites define the upper boundary and archaeocyatha the lower boundary of the Tommotian, whereas in the Iberian Peninsula trilobite occurrences predate archaeocyathid first appearance datums.

[13] Chronostratigraphical upper and lower age limits for the early Cambrian sechron of the Sierra de la Demanda are thus constrained by the age of the paleontologically dated Middle Cambrian basal beds from the overlying high-stand system tract and by the Ediacaran age of the rocks underneath [Liñán *et al.*, 1993, 2002; Valladares *et al.*, 2002a]. These imply that the sechron is bracketed between less than 542 ± 1 Ma and more than 525 Ma, if we consider that trilobites appeared before archaeocyatha marking the Tommotian – Atdabanian limit and take into account the age of tuffs interbedded with the oldest known archaeocyatha from Morocco [cf. Maloof *et al.*, 2010b], or between less than 542 ± 1 Ma and more than 520–521 Ma, if we follow the International Commission on Stratigraphy first appearance datum of trilobites.

4. Sample Description and U-Pb Results

4.1. The “Anguiano Conglomerate”

[14] The “Anguiano Conglomerate” is an up to 300 m thick siliciclastic succession made of conglomerates and minor sandstone intercalations (Figures 2 and 3a). It contains a modal proportion above 90% of monocrystalline (vein) quartz, chert and quartzite pebbles (Figure 3b), and can be considered a “quartz-pebble conglomerate” [Cox *et al.*, 2002]. Bed dips are moderate. The unit exhibits a thickness variation from 300 m in the eastern Sierra de la Demanda down to 30 m 20 km to the west, which implies an apparent angle $< 1^\circ$ between the base and the top contacts. The sedimentary structures observed and the internal organization in sequences disclose a coarse-grained gravel-rich coastal sedimentary environment. Likely, it was a gravel beach, taking into account diagnostic features such as the high degree of clast sorting, the segregation of gravel from

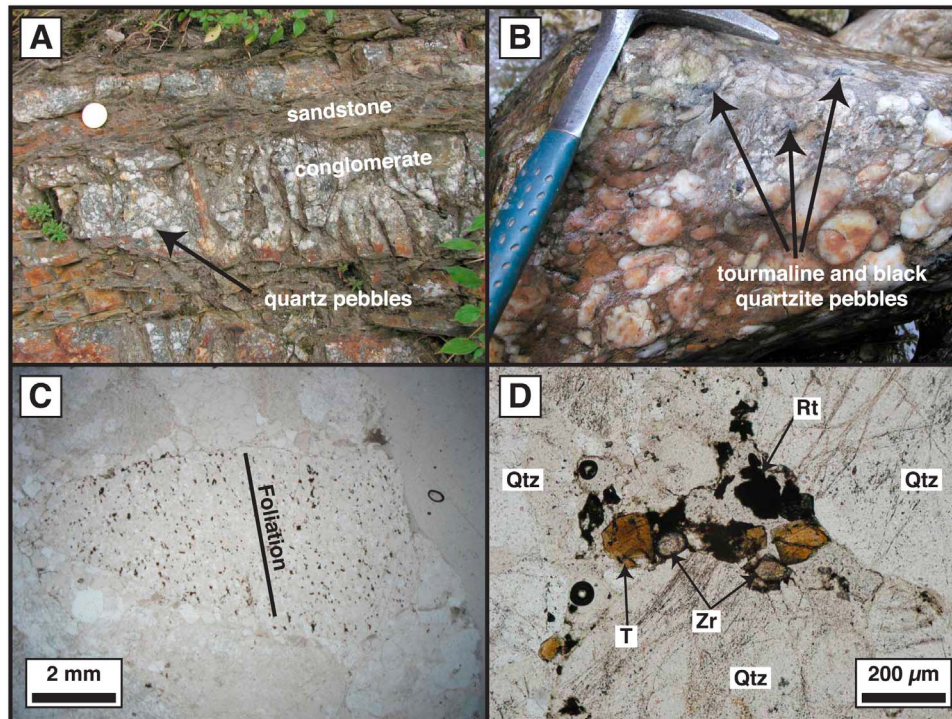


Figure 3. (a) Anguiano Conglomerate layers interbedded with sandstones in the lower part of the “Anguiano Conglomerate” (road talus, 1 km south of Anguiano). Note the occurrence of rounded quartz pebbles (white). (b) Close view of a conglomerate bed with centimeter-size, rounded quartzose pebbles and smaller, more irregular black pebbles (pointed by the arrows) of quartzite and tourmaline (Najerilla river course, 2 km south of Anguiano). (c) Photomicrograph (plane polarized light) of a metasandstone pebble containing abundant, minute dark minerals consisting of zircon, rutile and tourmaline. Note the alignment of the dark minerals and of the quartz grains (with variably intense white tones) defining a foliation (subperpendicular to the long edge of the micrograph). (d) Detail (plane polarized light) of the matrix between conglomerate pebbles showing heavy mineral concentrates (microplacers) of rutile (black grains), tourmaline (green-brown) and zircon (gray crystal with thick black rims). Abbreviations: rutile (Rt), tourmaline (T), quartz (Qtz), zircon (Zr).

sand, the lateral continuity of the beds, the rounding of the clasts and the horizontal lamination. The coarse grain size and the wedge shape of the formation indicate that the source area should be located not too far, to the East [Colchen, 1974], the physical connection between them likely corresponding to river-mouth/shelf-type delta transitions. Palinspastic restoration of Alpine north-verging displacement of the Sierra de la Demanda [Capote *et al.*, 2002] permits us to foresee that the source region of the conglomerate might eventually be located under its current outcrop, in the autochthon of the Iberian Ranges (the so-called Ebro Massif), covered by Phanerozoic successions and thrust slices.

[15] The conglomerate contains abundant, well-rounded silicic pebbles mm to cm in grain size (Figure 3b). The pebbles are of various types: metamorphic polycrystalline quartz aggregates, monocrystalline quartz, black chert, zircon-rutile- and tourmaline-bearing sandstone (Figure 3c) and foliated quartzite; white mica may also occur as inclusions, while biotite is exceedingly rare. Colchen [1974] also reported the occurrence of tourmalinite black pebbles with different microstructures in the basal part of the unit. The matrix is undeformed and contains much smaller monocrystalline quartz grains. Primary porosity was diagenetically

filled with quartzose precipitates that also cemented pebbles and matrix grains (pressure-solution microstructures and quartz grain syntaxial overgrowths). The matrix includes minor amounts of accessory zircon, tourmaline, rutile and mica (Figure 3d).

4.2. Zircon-Bearing Metasandstone Pebble Petrography

[16] Metaquartzite and metasandstone pebbles often show fabrics (continuous foliations and lattice preferred orientations) related to amphibolite facies and lower grade syn-tectonic metamorphism [Ábalos *et al.*, 2011]. Sandstone pebbles are made of quartz and less abundant feldspar grains embedded by a finer grained matrix with minor amounts of oriented mica and chlorite. These pebbles often contain detrital tourmaline, rutile and zircon grains (Figure 3c), in order of abundance, and, less commonly, muscovite and very rare biotite, pointing to either plutonic or medium- to high-grade metamorphic precursors. Zircons are often slightly to moderately rounded subhedral, detrital mineral grains (Figures 4a–4e). Some sandstone lithologies show zircon and rutile-rich layers. Here they are even observed as polycrystalline aggregates, likely because they were deposited as

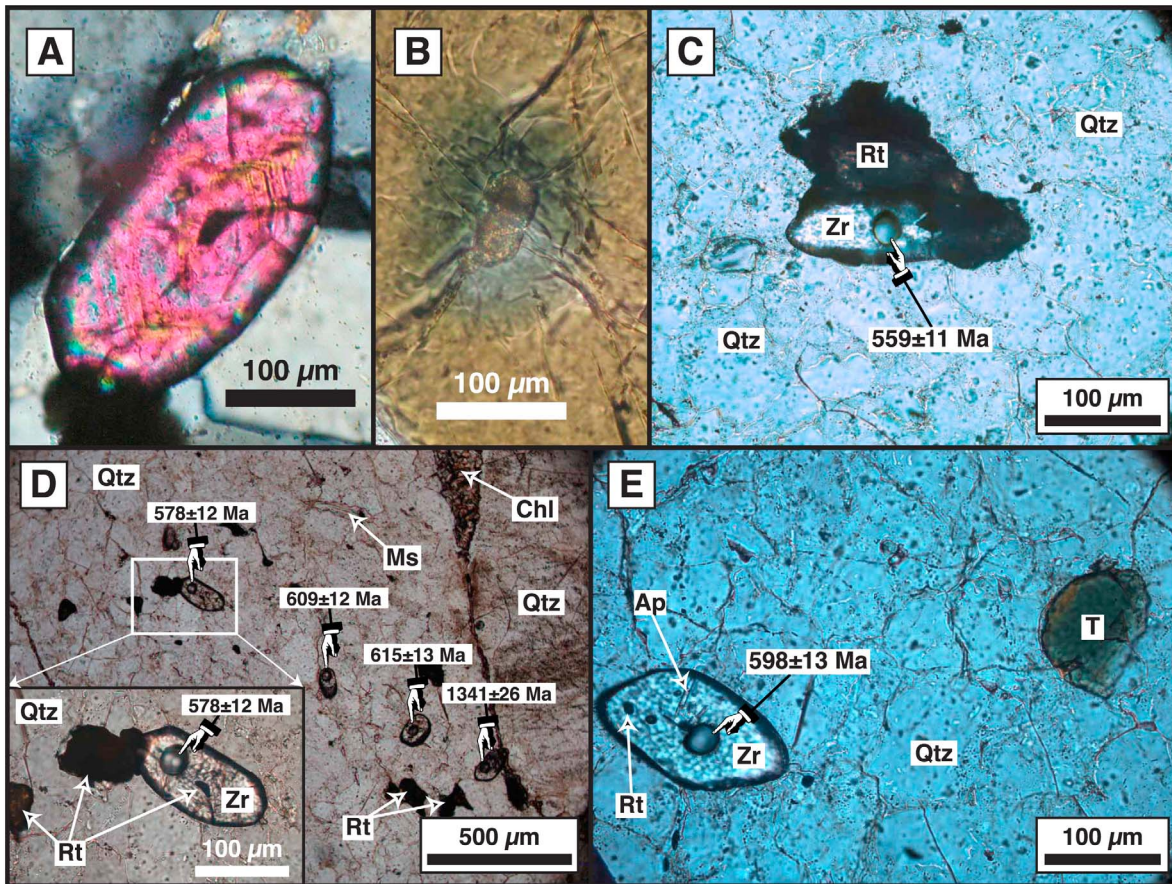


Figure 4. Optical micrographs of petrographic features supporting a zircon magmatic origin. Ablation spots and dating results ($^{206}\text{Pb}/^{238}\text{U}$ ages in Ma) show that zircons relate to Meso- and Neoproterozoic magmatism. (a) Crossed polar micrograph of a subidiomorphic zircon grain showing prism and pyramidal crystal faces with conspicuous growth zoning. (b) Plane polarized micrograph of a subhedral zircon grain with a haloed inclusion within a detrital tourmaline grain. (c) Micrograph of a zircon-rutile cluster from a metaquartzite pebble. The zircon grain provided the youngest concordant radiometric age (559 ± 11 Ma). (d) Plane polarized micrograph of a metasandstone pebble containing a millimeter size trail (running from top left to lower right) of zircon and rutile crystals. Also shown are a muscovite inclusion in the quartzite pebble and chlorite filling a fracture. The inset shows a detail of a zircon grain with rutile inclusions and growth zoning evidence. (e) Plane polarized micrograph of detrital tourmaline and zircon with idiomorphic inclusions of apatite. Abbreviations: rutile (Rt), tourmaline (T), apatite (Ap), quartz (Qtz), muscovite (Ms), chlorite (Chl).

microplacers (Figure 4d). Beach placer deposits can contain detrital heavy mineral concentrates that resulted from the erosion of large continental areas and are considered as a proxy for their average composition [Garçon *et al.*, 2011].

[17] Petrographic observations show that stubby and long prismatic zircon sections bear acicular prismatic inclusions of apatite (Figure 4e) and internal primary structures, such as prism and pyramidal crystal faces with conspicuous growth zoning (Figure 4a). This suggests magmatic zircon growth prior to limited abrasion during erosion and sedimentary transport. A subhedral zircon grain has been found as a haloed inclusion within a detrital tourmaline grain (Figure 4b). This might suggest that magmatic, metamorphic overprinted and sedimentary recycled zircons concurred during conglomerate deposition.

4.3. Analytical Methods: LA-ICP-MS U-Pb Zircon Dating

[18] The occurrence of zircon-rich layers in the quartzite pebbles allowed the zircons, one to two points depending on the crystal size, to be analyzed without difficulty on polished petrographic thin sections (e.g., Figures 4c–4e). U-Th-Pb geochronology of zircon was conducted by laser ablation inductively coupled plasma mass spectrometry (LA-ICP-MS). Two quadrupole-based ICP-MS instruments and two different laser systems were used in this work.

[19] At the Laboratoire Magmas et Volcans, Clermont-Ferrand (France), the analyses involved the ablation of minerals in ca. $30 \mu\text{m}$ thick petrographic sections with a Resonetics Resolution M-50 powered by an ultra short pulse ATL Atlex Excimer laser system operating at a wavelength of 193 nm (detailed description in Müller *et al.* [2009]).

Table 1. Operating Conditions of Laser Ablation ICP-MS

ICPMS System	Agilent 7500 cs	Thermo XSeries 2
RF power	1350 W	1350 W
Nebulizer gas flow (Ar) (optimized daily)	ca. 0.85 l/min	ca. 0.90 l/min
Coolant gas flow	16 l/min	14.9 l/min
Auxiliary gas flow	1 l/min	0.9 l/min
Data acquisition protocol	Time-resolved analysis	
Scanning mode	Peak jumping, 1 point per peak	
Detector mode	Pulse counting, dead time correction applied, and analog mode when signal intensity > 1 million CPS	
Isotopes acquired	²⁰² Hg, ²⁰⁴ (Hg+Pb), ²⁰⁶ Pb, ²⁰⁷ Pb, ²⁰⁸ Pb, ²³² Th, ²³⁸ U	
Dwell time per isotope	10–30 ms	10–20 ms
Sampler, skimmer cones	Ni	
Laser-Ablation System	Resonetics Resolution M-50E	New Wave UP213
Laser type/wavelength	Excimer 193 nm	Nd:YAG 213 nm
Pulse duration	<4 ns	3–5 ns
Energy density on target	ca. 9 J/cm ²	ca. 5 J/cm ²
ThO ⁺ /Th ⁺		<0.05%
He gas flow	0.75 l/min	0.9–1 l/min
N ₂ gas flow	7 ml/min	-
Laser repetition rate	4 Hz	10 Hz
Laser spot size	20–26 μm	25 μm
Acquisition time (blank+ablation)	30 s + 60 s	

Spot diameters of 20 and 26 μm associated to repetition rates of 4 Hz and laser energy of 4 mJ producing a fluence of 9 J/cm² were used for zircon dating. The ablated material was carried into helium, and then mixed with nitrogen and argon, before injection into a plasma source of an Agilent 7500 cs ICP-MS equipped with a dual pumping system to enhance the sensitivity. Table 1 summarizes the operating conditions of the laser ablation ICP-MS apparatus.

[20] The alignment of the instrument and mass calibration was performed before every analytical session using the NIST SRM 612 reference glass, by inspecting the signal of ²³⁸U and by minimizing the ThO⁺/Th⁺ ratio (<1%). The mean sensitivity on ²³⁸U at the instrumental conditions reported in Table 1 and using a spot size of 44 μm is about 15–20,000 cps/ppm. The analytical method for isotope dating with laser ablation ICP-MS is basically similar to that developed for zircon and monazite and reported in *Tiepolo* [2003] and *Paquette and Tiepolo* [2007]. The signals of ²⁰⁴(Pb+Hg), ²⁰⁶Pb, ²⁰⁷Pb, ²⁰⁸Pb, ²³²Th and ²³⁸U masses were acquired. The occurrence of common Pb in the samples can be monitored by the evolution of ²⁰⁴(Pb+Hg) signal intensity, but no common Pb correction was applied owing to the large isobaric interference from Hg. The ²³⁵U signal was calculated from ²³⁸U on the basis of the ratio ²³⁸U/²³⁵U = 137.88. Single analyses consisted of 30 s of background integration with laser off followed by 60 s integration with the laser firing and a 30 s delay to wash out the previous sample (approximately 10 s for 6 orders of magnitude) and prepare the next analysis.

[21] At the Geochronology and Isotope Geochemistry of the SGIker-University of the Basque Country (Spain) the analyses involved the ablation of minerals in ca. 60 μm thick petrographic sections with an UP213 frequency quintupled Nd:YAG based laser ablation system (NewWave Research, Fremont, USA) coupled to a Thermo Fisher Scientific Xseries 2 quadrupole based ICP-MS instrument with enhanced sensitivity through a dual pumping system. Instrument and operating parameters used for individual

zircon analyses fell within the parameters given in Table 1. Spot diameters of 25 μm associated to repetition rates of 10 Hz and laser fluence at the target of ca. 5 J/cm² were used for zircon dating. The ablated material was carried into helium and then mixed with argon, before injection into the plasma source. Tuning and mass calibration were performed following a similar procedure as in Clermont-Ferrand except for the spot sizes of 100 μm to obtain ca. 40,000 cps/ppm on ²³⁸U in the NIST SRM 612 glass.

[22] Data were corrected in both cases for U-Pb and Th-Pb fractionation occurring during laser sampling and for instrumental mass discrimination (mass bias) by standard bracketing with repeated measurements of GJ-1 zircon standard [*Jackson et al.*, 2004]. At the beginning and at the end of every run, repeated analyses of 91500 zircon standard [*Wiedenbeck et al.*, 1995], treated as unknowns, independently controlled the reproducibility and accuracy of the corrections. Data reduction was carried out with the software package GLITTER® [*van Achterbergh et al.*, 2001; *Jackson et al.*, 2004]. For each analysis, the time resolved signal of single isotopes and isotope ratios was monitored and carefully inspected to verify the presence of perturbations related to inclusions, fractures, mixing of different age domains or common Pb. Calculated ratios were exported and Concordia ages and diagrams were generated using the Isoplot/Ex v. 2.49 software package [*Ludwig*, 2001]. The concentrations in U-Th-Pb were calibrated relative to the certified contents of GJ-1 zircon standard [*Jackson et al.*, 2004]. Percentage concordance was calculated as [(²⁰⁶Pb/²³⁸U age)/(²⁰⁷Pb/²⁰⁶Pb age)] × 100.

4.4. U-Pb Zircon Age Spectra

[23] One hundred and sixty U-Pb analytically valid analyses were selected from more than two hundred spot measurements performed in one hundred zircons. Elemental and isotopic data are presented in order of increasing ²⁰⁶Pb/²³⁸U ages in Table 2 (SD-labeled data were obtained with the UP213-XSeries set up and other data with the 193 Excimer-

Table 2. LA-ICP-MS U-Th-Pb Data of Zircons From Quartzite Pebbles in the Anguiano Conglomerate, Sierra de La Demanda

Number	Spot	Pb (ppm)	U (ppm)	Th/U	$^{207}\text{Pb}/^{235}\text{U}$	$\pm 2\sigma$	$^{206}\text{Pb}/^{238}\text{U}$	$\pm 2\sigma$	$^{206}\text{Pb}/^{238}\text{U}$ Age (Ma)	$\pm 2\sigma$	Concentration (%)
1	09290610c	221	5239	0.5	0.6720	0.0149	0.0354	0.0008	224	5	10
2	27290610c	104	2200	1.1	0.4974	0.0122	0.0393	0.0008	249	3	17
3	39290610c	98	1891	1.1	0.6606	0.0160	0.0431	0.0009	272	6	15
4	18300610c	44	1023	0.1	0.3472	0.0108	0.0453	0.0010	286	6	66
5	19300610c	29	632	0.5	0.3762	0.0173	0.0454	0.0010	286	6	47
6	22290610b	128	1895	0.7	10.456	0.0241	0.0496	0.0010	312	6	13
7	29290610c	130	2172	0.7	0.5724	0.0137	0.0532	0.0011	334	7	29
8	SD322IVD3	167	4353	0.95	0.9790	0.0182	0.0580	0.0009	364	5	18
9	08300610b	1526	1945	42.5	0.4755	0.0119	0.0595	0.0012	372	8	70
10	SD322IVD6	38	952	0.51	0.6524	0.0204	0.0628	0.0011	392	7	36
11	SD323	51	1407	0.21	0.6259	0.0150	0.0633	0.0010	396	6	40
12	30290610c	74	980	1	0.6892	0.0186	0.0641	0.0014	401	8	35
13	SD322IVD7	20	379	0.85	10.104	0.0471	0.0693	0.0018	432	11	25
14	20290610c	48	538	1.1	0.6560	0.0215	0.0721	0.0016	449	10	56
15	SD28B1	17	439	0.15	0.7213	0.0417	0.0726	0.0019	452	12	46
16	SD34	3	54	1.01	0.6084	0.0415	0.0728	0.0026	453	16	72
17	37290610c	80	1050	0.4	0.6702	0.0173	0.0735	0.0016	457	10	57
18	11300610c	14	199	0.2	0.5872	0.0221	0.0738	0.0016	459	10	89
19	SD26A3	119	2822	0.29	0.6632	0.0169	0.0746	0.0012	464	7	61
20	18290610b	22	270	0.6	0.7283	0.0229	0.0747	0.0016	465	10	49
21	19290610c	16	184	0.7	0.7028	0.0380	0.0779	0.0019	483	12	61
22	SD2175	153	2801	0.67	0.7592	0.0177	0.0779	0.0013	483	8	51
23	SD220b	137	2698	0.49	0.8434	0.0182	0.0780	0.0013	484	8	42
24	SD235	134	2874	0.45	0.9696	0.0329	0.0789	0.0016	489	9	35
25	SD322IIC2a	211	4078	0.18	0.6672	0.0209	0.0790	0.0014	490	8	76
26	SD2181	44	924	0.19	0.7330	0.0181	0.0793	0.0013	492	8	59
27	12300610b	417	1010	3.0	0.6701	0.0191	0.0796	0.0017	494	10	77
28	17290610b	28	270	1.4	0.7739	0.0322	0.0802	0.0019	497	11	54
29	SD31B	12	214	0.27	0.6942	0.0268	0.0802	0.0022	497	13	70
30	06300610c	9	100	0.6	0.6642	0.0414	0.0802	0.0020	497	12	82
31	34290610c	41	474	0.5	0.6668	0.0174	0.0811	0.0017	503	10	85
32	05300610c	14	142	0.9	0.6906	0.0338	0.0814	0.0019	505	11	77
33	10290610b	65	783	0.4	0.7306	0.0180	0.0816	0.0017	506	10	66
34	25300610b	31	329	1.0	0.6646	0.0252	0.0818	0.0018	507	11	90
35	SD28B2	132	2621	0.52	0.6871	0.0133	0.0834	0.0013	517	8	87
36	SD28A5	251	4041	1.08	0.7524	0.0270	0.0835	0.0016	517	10	66
37	SD322IIIA3	44	689	0.68	0.6719	0.0463	0.0836	0.0023	518	14	96
38	16300610c	6	56	1.0	0.7455	0.0512	0.0840	0.0021	520	12	69
39	SD215	60	1037	0.63	0.7960	0.0215	0.0847	0.0015	524	9	60
40	SD26A4	27	487	0.45	10.065	0.0431	0.0850	0.0019	526	11	39
41	20290610b	24	242	0.9	0.7351	0.0273	0.0857	0.0019	530	11	78
42	16290610b	43	372	1.7	0.8727	0.0238	0.0862	0.0019	533	11	52
43	SD322IIIC6	172	2721	0.55	0.8347	0.0221	0.0864	0.0014	534	8	58
44	SD322IVB2	174	1928	2.87	0.7581	0.0171	0.0868	0.0014	537	8	75
45	16300610b	88	971	0.3	10.082	0.0285	0.0870	0.0018	538	11	42
46	SD211	85	1632	0.15	0.7406	0.0190	0.0874	0.0015	540	9	82
47	29300610b	14	140	0.8	0.7597	0.0277	0.0879	0.0019	543	11	78
48	SD36A	48	753	0.51	0.7367	0.0194	0.0883	0.0019	545	12	89
49	SD36	6	108	0.23	0.7953	0.0298	0.0886	0.0019	547	11	69
50	20300610b	86	645	2.3	0.8005	0.0248	0.0890	0.0019	550	11	70
51	18290610c	19	211	0.4	0.7634	0.0243	0.0895	0.0020	553	12	83
52	SD322IVB3	64	1302	0.14	0.7630	0.0179	0.0896	0.0014	553	8	83
53	07300610c	45	400	1.3	0.7499	0.0208	0.0899	0.0019	555	11	89
54	09300610b	29	291	0.7	0.7736	0.0256	0.0899	0.0019	555	11	81
55	SD2178	81	1372	0.66	0.9902	0.0349	0.0901	0.0018	556	11	47
56	SD292	64	1052	0.88	0.7656	0.0244	0.0901	0.0016	556	10	84
57	49290610c	6	51	1.7	0.7362	0.0448	0.0905	0.0022	558	13	98
58	15300610b	18	188	0.6	0.7866	0.0340	0.0905	0.0020	559	12	79
59	07290610b	43	500	0.1	0.7457	0.0180	0.0909	0.0019	561	11	96
60	SD28A2	79	1453	0.50	0.8220	0.0221	0.0909	0.0015	561	9	71
61	25290610c	31	315	0.6	0.7520	0.0241	0.0910	0.0020	562	12	94
62	10300610c	14	149	0.2	11.293	0.0741	0.0918	0.0025	566	15	40
63	SD322IIIC8	78	1246	0.28	0.7494	0.0302	0.0919	0.0018	567	10	100
64	SD32A	39	550	0.72	0.7609	0.0198	0.0921	0.0017	568	10	96
65	30290610b	10	92	0.7	0.7636	0.0329	0.0926	0.0021	571	12	95
66	19290610b	11	93	1.4	0.7984	0.0258	0.0930	0.0020	573	12	84
67	31290610b	54	511	0.8	0.7846	0.0198	0.0938	0.0020	578	12	92
68	SD322IVC4	175	3192	0.34	0.7933	0.0141	0.0939	0.0014	579	8	89
69	08300610c	10	94	0.7	0.8162	0.0367	0.0940	0.0021	579	12	82
70	SD322IVB1	53	982	0.28	0.8328	0.0258	0.0940	0.0017	579	10	77
71	SD322IVD2	38	523	1.47	0.8132	0.0280	0.0942	0.0017	581	10	84

Table 2. (continued)

Number	Spot	Pb (ppm)	U (ppm)	Th/U	$^{207}\text{Pb}/^{235}\text{U}$	$\pm 2\sigma$	$^{206}\text{Pb}/^{238}\text{U}$	$\pm 2\sigma$	$^{206}\text{Pb}/^{238}\text{U}$ Age (Ma)	$\pm 2\sigma$	Concentration (%)
72	45290610c	11	115	0.3	0.9803	0.0489	0.0946	0.0023	583	14	54
73	SD322IC3	14	181	0.99	0.7805	0.0310	0.0948	0.0019	584	11	99
74	13300610b	8	75	0.7	0.7894	0.0528	0.0949	0.0024	584	14	95
75	SD322IIC2c	33	542	0.19	0.8089	0.0410	0.0952	0.0022	586	13	89
76	14290610c	213	2024	0.4	17.499	0.0400	0.0960	0.0021	591	12	28
77	17290610c	85	804	0.9	10.098	0.0243	0.0971	0.0021	598	12	55
78	26300610b	7	64	0.9	0.8617	0.0392	0.0972	0.0022	598	13	80
79	SD31C	8	122	0.33	0.8940	0.1543	0.0978	0.0018	601	11	71
80	40290610c	18	170	0.7	0.8206	0.0293	0.0979	0.0022	602	13	95
81	25290610b	31	271	0.8	0.8384	0.0218	0.0982	0.0021	604	12	90
82	24300610b	18	182	0.3	0.8216	0.0277	0.0985	0.0021	606	12	98
83	32290610b	48	395	1.1	0.8693	0.0224	0.0991	0.0021	609	12	84
84	26290610b	34	309	0.6	0.9720	0.0350	0.0996	0.0022	612	13	64
85	35290610b	14	140	0.4	0.8336	0.0231	0.1001	0.0021	615	13	100
86	17300610b	14	140	0.3	0.8713	0.0350	0.1001	0.0022	615	13	86
87	27290610b	66	653	0.3	0.8534	0.0205	0.1010	0.0021	621	13	96
88	SD322IIB2	47	537	1.06	0.8791	0.0413	0.1015	0.0022	623	13	89
89	09300610c	36	261	1.5	0.8732	0.0241	0.1019	0.0021	626	12	92
90	SD322IIB1	40	471	0.87	0.8581	0.0497	0.1028	0.0026	631	15	101
91	35290610c	40	471	0.9	0.9394	0.0264	0.1028	0.0022	631	7	77
92	SD2177	20	291	0.52	15.082	0.0558	0.1039	0.0023	637	13	37
93	06290610c	39	380	0.2	0.9132	0.0247	0.1046	0.0023	642	13	89
94	55290610c	36	319	0.6	0.9275	0.0255	0.1058	0.0023	648	13	89
95	07300610b	81	806	0.1	0.9915	0.0263	0.1061	0.0022	650	13	75
96	SD322IIIA1	61	900	0.32	0.9128	0.0335	0.1068	0.0020	654	12	97
97	SD322IIB4a	27	292	1.05	0.9141	0.0498	0.1073	0.0026	657	15	99
98	SD322IIC2b	39	565	0.18	0.8946	0.0300	0.1075	0.0019	658	11	107
99	41290610c	44	373	0.7	0.9544	0.0252	0.1080	0.0023	661	14	89
100	54290610c	42	571	0.2	0.9645	0.0367	0.1097	0.0025	671	14	91
101	SD322IIID2	42	571	0.21	0.9419	0.0461	0.1103	0.0024	675	14	101
102	SD322IIB4b	29	329	1.03	0.9498	0.0662	0.1111	0.0032	679	19	101
103	29290610b	39	326	0.5	11.962	0.0340	0.1112	0.0024	680	14	59
104	SD322IIB1	14	173	0.66	0.9666	0.0382	0.1115	0.0022	682	13	97
105	26290610c	21	172	0.6	0.9796	0.0307	0.1117	0.0025	683	14	94
106	SD322IIA1	47	620	0.29	13.393	0.0391	0.1129	0.0020	690	11	52
107	22300610b	47	378	0.5	10.586	0.0293	0.1171	0.0024	714	14	90
108	SD322IIID1	217	2226	0.90	13.660	0.0382	0.1172	0.0019	714	11	55
109	05290610c	7	47	1.5	11.810	0.0621	0.1178	0.0029	718	17	71
110	SD2184	31	396	0.34	11.531	0.0353	0.1227	0.0023	746	13	86
111	SD31A	18	238	0.16	10.939	0.0238	0.1232	0.0021	749	12	99
112	49290610c	6	51	1.7	0.7362	0.0448	0.0905	0.0022	558	13	98
113	47290610c	113	810	0.6	12.958	0.0334	0.1266	0.0027	768	16	73
114	50290610c	56	402	0.6	11.814	0.0318	0.1273	0.0028	773	16	91
115	SD322IVC1	128	1560	0.65	12.504	0.0258	0.1275	0.0020	774	11	81
116	SD322IIC7	95	916	0.88	11.854	0.0424	0.1288	0.0024	781	14	94
117	SD322IVA1A	12	124	0.39	23.751	0.1810	0.1320	0.0056	799	32	38
118	12290610b	18	128	0.5	12.071	0.0383	0.1329	0.0029	805	17	100
119	46290610c	43	299	0.4	12.934	0.0355	0.1380	0.0030	834	17	96
120	SD322IIA2	57	510	0.46	18.678	0.0855	0.1413	0.0034	852	19	55
121	SD35	28	268	0.60	13.939	0.0355	0.1415	0.0026	853	15	88
122	SD2162	47	404	1.32	14.783	0.0406	0.1429	0.0026	861	14	81
123	15290610b	26	169	0.5	13.421	0.0375	0.1443	0.0031	869	18	102
124	44290610c	58	382	0.4	14.166	0.0355	0.1452	0.0031	874	9	92
125	21290610c	78	344	2.3	14.664	0.0352	0.1471	0.0032	884	18	89
126	11300610b	34	232	0.2	14.499	0.0395	0.1476	0.0031	888	17	92
127	21300610b	55	318	0.5	24.407	0.0667	0.1508	0.0032	906	18	47
128	SD2183	53	501	0.70	15.780	0.0350	0.1516	0.0025	910	14	84
129	SD322IIID9	127	1145	0.37	15.047	0.0455	0.1537	0.0026	922	14	97
130	SD2185	35	317	0.79	16.428	0.0406	0.1541	0.0027	924	15	82
131	SD322IVD9	248	2921	0.05	16.972	0.0367	0.1562	0.0025	936	14	80
132	SD322IIC1b	297	2325	0.94	15.851	0.0490	0.1582	0.0028	947	16	94
133	20300610c	20	93	1.5	17.683	0.0743	0.1586	0.0036	949	20	78
134	14300610b	69	366	1.0	16.386	0.0508	0.1615	0.0035	965	19	94
135	31290610c	27	138	0.9	16.392	0.0455	0.1635	0.0036	976	20	97
136	27300610b	20	108	0.8	16.761	0.0542	0.1650	0.0035	984	19	95
137	12300610c	29	160	0.6	16.537	0.0454	0.1654	0.0035	987	19	99
138	38290610c	27	140	0.8	18.235	0.0512	0.1659	0.0036	989	20	83
139	28290610b	24	131	0.5	19.514	0.0615	0.1675	0.0037	998	20	77
140	10300610b	28	159	0.4	17.202	0.0461	0.1682	0.0035	1002	20	96
141	SD322IIC1a	156	1176	0.76	17.755	0.0594	0.1742	0.0032	1035	18	100
142	16290610c	29	138	0.8	19.285	0.0500	0.1835	0.0040	1086	22	99

Table 2. (continued)

Number	Spot	Pb (ppm)	U (ppm)	Th/U	$^{207}\text{Pb}/^{235}\text{U}$	$\pm 2\sigma$	$^{206}\text{Pb}/^{238}\text{U}$	$\pm 2\sigma$	$^{206}\text{Pb}/^{238}\text{U}$ Age (Ma)	$\pm 2\sigma$	Concentration (%)
143	11290610c	50	197	0.9	39.198	0.0950	0.2111	0.0046	1235	24	57
144	SD322IVD5	375	2627	0.47	33.560	0.0577	0.2264	0.0034	1316	18	75
145	SD322IVD4	456	3081	1.15	56.722	0.0945	0.2276	0.0034	1322	18	50
146	SD26A5	397	2700	0.17	51.100	0.0908	0.2544	0.0039	1461	20	64
147	SD322IID3	31	147	0.84	33.315	0.1316	0.2572	0.0055	1475	28	98
148	SD322IID5a	141	648	0.67	42.277	0.1428	0.2711	0.0052	1547	26	84
149	SD322IVD8	415	1901	0.92	76.678	0.1318	0.2842	0.0043	1613	22	58
150	SD322IID5b	149	605	0.74	51.116	0.1995	0.3021	0.0066	1702	33	85
151	17300610c	70	196	0.8	47.257	0.1228	0.3042	0.0063	1712	31	93
152	SD2121	80	366	0.44	58.532	0.1216	0.3246	0.0055	1812	27	86
153	SD322IC5	68	242	0.53	63.726	0.1613	0.3695	0.0062	2027	29	100
154	SD26B1	169	707	0.27	103.266	0.2007	0.3773	0.0062	2063	29	73
155	SD322IVD1	92	376	0.41	82.127	0.1468	0.3817	0.0059	2084	27	86
156	SD322IIB2	358	1368	0.23	80.983	0.1937	0.3900	0.0067	2123	31	90
157	05300610b	143	299	0.4	114.411	0.2653	0.4221	0.0089	2270	40	81
158	SD242	11	31	0.31	172.646	10.048	0.4410	0.0213	2355	95	70
159	SD322IVC3	48	136	1.08	111.768	0.1977	0.4788	0.0074	2522	32	99
160	SD322IVD10	263	852	0.28	126.056	0.2137	0.4882	0.0074	2563	32	94

7500 set up). These zircons exhibit large ranges of Pb, Th and U contents, most of them bearing Th/U ratios of 0.5 to 0.9, typical of magmatic origin.

[24] Representative U-Pb concordia diagrams (Figures 5 and 6) show the results of LA-ICP-MS dating with 2σ errors for the ellipses (decay-constant errors included). The calculated ages ($^{206}\text{Pb}/^{238}\text{U}$) range from 224 Ma to 2563 Ma, but the majority are from ca. 550 Ma to 1000 Ma (Table 2). While many of the oldest and youngest zircons are discordant, possibly because of Pb loss in Paleoproterozoic or subsequent times, Neoproterozoic zircons are mostly

concordant or sub-concordant (Figure 6). Most of the discordant zircons would lie along hypothetical discordia lines yielding upper intercept ages ranging between ca. 1800 Ma and more than 2800 Ma, and cluster at similar lower intercepts of Upper Neoproterozoic age (dashed lines in Figure 5), suggesting nonzero Pb loss. Nonetheless, and since it is impossible to establish whether these are either real discordances, the effect of common Pb or just undetected analytical/mineralogical artifacts (inclusions, cracks, different Zr domains, etc.), in the sections below the discussion will be focused only on the concordant or sub-

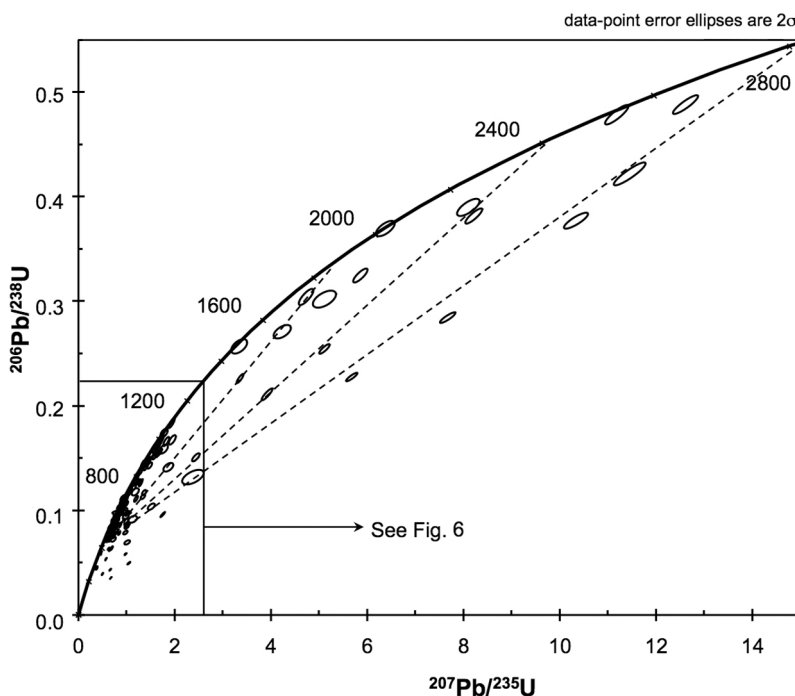


Figure 5. U-Pb concordia diagram for the original set of analyses from the Anguiano quartz pebble conglomerate. Dashed segments are hypothetical discordia lines yielding upper intercept ages ranging between ca. 1800 Ma and more than 2800 Ma, and lower intercepts of Upper Neoproterozoic age. Data-point error ellipses are 2σ .

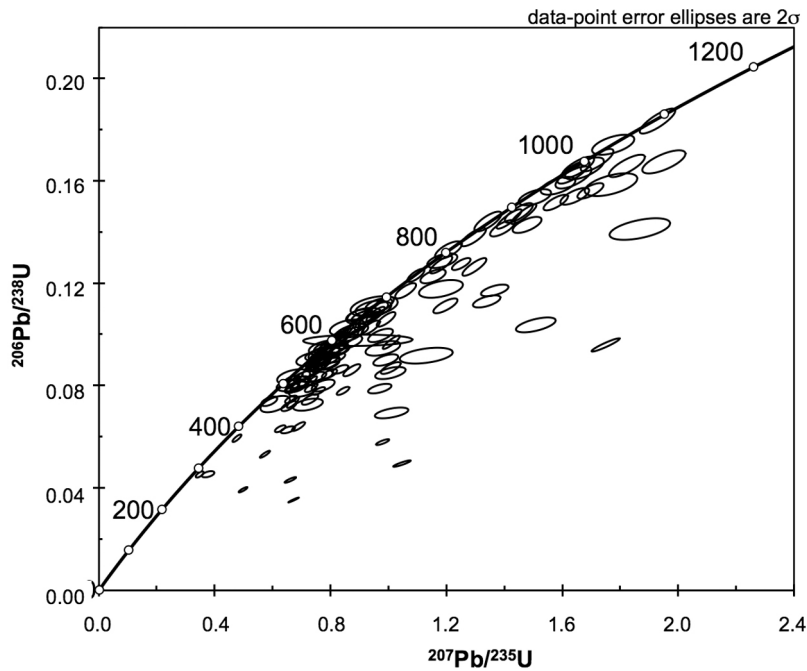


Figure 6. Close-up view of Figure 5. U-Pb concordia diagram showing the clusters of concordant Neoproterozoic and late Mesoproterozoic ages.

concordant data, and it will be assumed that most ages >2.0 Ga are just minimum apparent ages.

[25] In the Figure 7 an alternative data presentation in a Tera-Wasserburg diagram [Tera and Wasserburg, 1973] is provided. It shows the inheritance characteristics of the zircons studied and virtually absent discordia lines. The diagram permits to disclose various concordant zircon age populations (clustered around 2700–2500, 2300, 2100–

2000, 1500, 1000 and 600 Ma). From them, the 2100–2000, 1000 and 600 Ma clusters are the best defined and most representative (see inset in Figure 7).

[26] Concordant to nearly concordant zircon spots analyzed exhibit $^{206}\text{Pb}/^{238}\text{U}$ age spectra with various frequency maxima (Figure 8). The probability density histogram plots show that the population of zircons younger than 1200 Ma, with concordance $>90\%$ ($n = 51$), can be divided into three

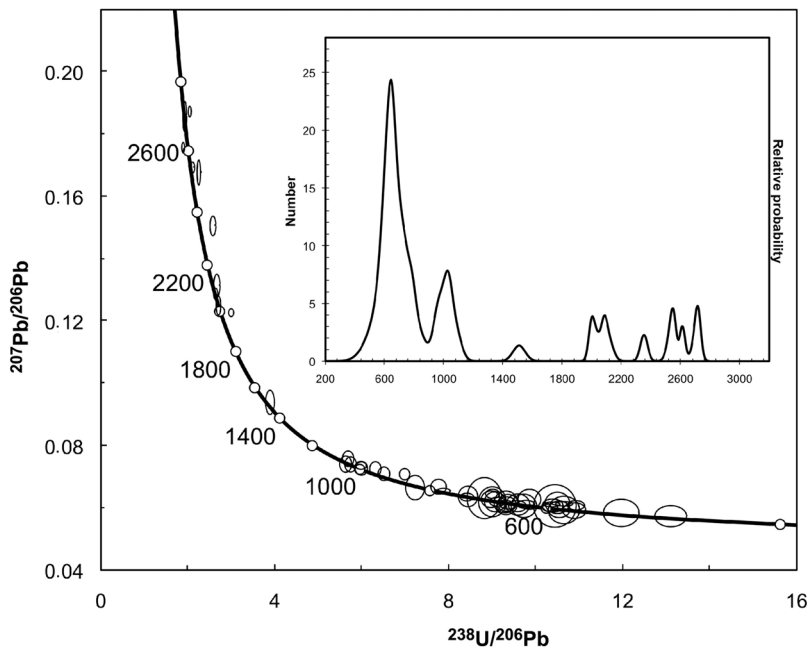


Figure 7. Tera-Wasserburg diagram for the concordant and nearly concordant zircons studied. Data-point error ellipses are 2σ . The corresponding probability density plot is presented in the inset.

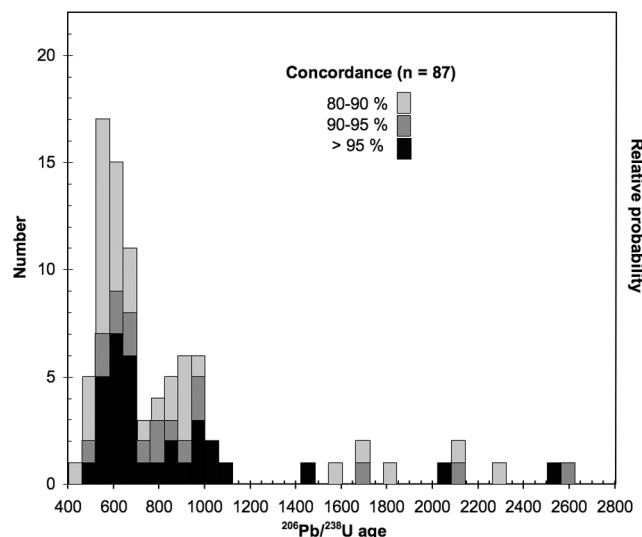


Figure 8. Histogram of concordant to nearly concordant zircon ages spectra; 87 spots yielded $^{206}\text{Pb}/^{238}\text{U}$ ages with concordance >80%, 51 > 90% and 33 > 95%. See text for details.

main groups, apart from an older, less represented population. These four age groups are dealt with in detail below. They can also be identified, albeit less precisely, when the population of zircons with concordance over 80% ($n = 87$) are taken into account (Figure 8).

[27] Nearly 10% of the zircons analyzed yielded late Neoproterozoic (2.56–2.52 Ga) to Paleoproterozoic (2.27–1.70 Ga) and rare early Mesoproterozoic (1.54–1.47 Ga) ages. Most of them are concordant or sub-concordant $^{206}\text{Pb}/^{238}\text{U}$ – $^{207}\text{Pb}/^{206}\text{Pb}$ ages. An age group comprising nearly 8% of the zircons analyzed and relates to the latest orogenically active period of the Mesoproterozoic, the Stenian (1.2 to 1.0 Ga). Concordant or nearly concordant $^{206}\text{Pb}/^{238}\text{U}$ ages of this group (less than 1% discordant) range between 1086 ± 22 and 1035 ± 18 Ma, and less concordant ages extended down to 987 ± 19 or 976 ± 20 Ma. Early and Middle Neoproterozoic age populations have frequencies of 11 and 20%, respectively. The former group (Tonian, lasting from 1000 to 850 Ma) contains mostly nearly concordant $^{206}\text{Pb}/^{238}\text{U}$ ages in the range 922 ± 14 – 869 ± 18 Ma. The second group (Cryogenian, from 850 to 635 Ma) is represented by several concordant ages ranging from 805 ± 17 to 675 ± 14 Ma (Table 2). The late Neoproterozoic (Ediacaran) is represented by ca. 45% of the zircon data. Two data subsets of similar frequency can be distinguished: a first group in the range 631 ± 50 – 584 ± 11 Ma and a second one in the 571 ± 12 – 558 ± 13 Ma interval. Both groups include several concordant or nearly concordant (>95%) $^{206}\text{Pb}/^{238}\text{U}$ ages (see Table 2).

5. Discussion

[28] The wealth of radiometric ages recovered from inherited detrital zircon grains from different parts of the Iberian Massif has provided accurate time constraints on the source regions of the Neoproterozoic sedimentary basin [Fernández-Suárez *et al.*, 2000, 2002, 2003; Gutiérrez-

Alonso *et al.*, 2005]. These relate notably to Neoproterozoic (Pan-African and Cadomian) orogens and, to a lesser extent, to Paleoproterozoic (1.8–2.1 Ga) or Neoproterozoic (2.4–2.8 Ga) ones that resemble the West-African craton [e.g., Nögler *et al.*, 1995; Ugidos *et al.*, 1997; Valladares *et al.*, 2002b].

[29] Mesoproterozoic relics of possible non-Gondwanan affinity were found in units of exotic origin (allochthonous) with respect to the Iberian Massif and in autochthon, Neoproterozoic to early Paleozoic sedimentary successions [e.g., Fernández-Suárez *et al.*, 2003; Gutiérrez-Alonso *et al.*, 2005; Sánchez-Martínez *et al.*, 2006, 2011; Abati *et al.*, 2010]. Relics of that age have also been found in Paleozoic sediments of North Africa [Linnemann *et al.*, 2011]. In the Arabian-Nubian Shield area [Avigad *et al.*, 2003; Morag *et al.*, 2011a, 2011b] they are derived from late Neoproterozoic rocks of northeastern Africa and can thus be considered of Gondwanan affinity (Figure 9). In the Tuareg Shield area the source rocks are thought to occur outside the West African area, the Amazon craton being a potential candidate [cf. Linnemann *et al.*, 2011].

[30] The zircon age spectra described in this study (Table 2 and Figures 5–8) will be discussed below from various complementary perspectives. First we shall deal with its use to constrain the duration of sedimentation during deposition of the early Cambrian transgressive system tract. Then we shall discuss the organization of the continental mass whose detritus were deposited in the Neoproterozoic Iberian sedimentary basin. This discussion has two perspectives, in regard to the Neoproterozoic and Mesoproterozoic paleotectonic settings, on one hand, and to the paleo-surface geology of the continental mass, on the other hand (Figure 9). Finally, we propose a likely source region for the conglomerate and detrital zircons studied.

5.1. Maximum Depositional Age of the Early Cambrian Sechron

[31] The youngest cluster of subconcordant $^{206}\text{Pb}/^{238}\text{U}$ Ediacaran ages is 558 ± 13 Ma (less than 2% discordant zircon age, MSWD = 0.026). A younger, near concordant (96%) age of 518 ± 14 Ma was obtained, too (Table 2). These are late Ediacaran to early Cambrian ages, since even with their error margins they may be considered older (the first ages) or younger (the second one) than the 542 ± 1 Ma age of the Ediacaran–Cambrian boundary. The former ages represent with confidence the maximum depositional age of the Anguiano Conglomerate, though the 518 ± 14 Ma might do the job as well. The fact that the depositional age should be younger is demonstrated by the two erosion-sedimentation cycles implied by the incorporation of the metasandstone pebbles with zircon-rutile microplacers to the conglomerate. These results would modify toward the younger ages (within the error margins) the time constraints for the initiation of the early Cambrian sechron of the Sierra de la Demanda provided by regional stratigraphic and paleontologic correlations. According to them, the base of the Cambrian should be older than 525 Ma or 520–521 Ma. Geochronology prompts that simultaneously it should be younger than 532 Ma ($518 + 14$ Ma). This would demonstrate the occurrence of an earliest Cambrian hiatus in the Sierra de la Demanda, between the unconformable basal contact of the early Cambrian sechron and the underlying,

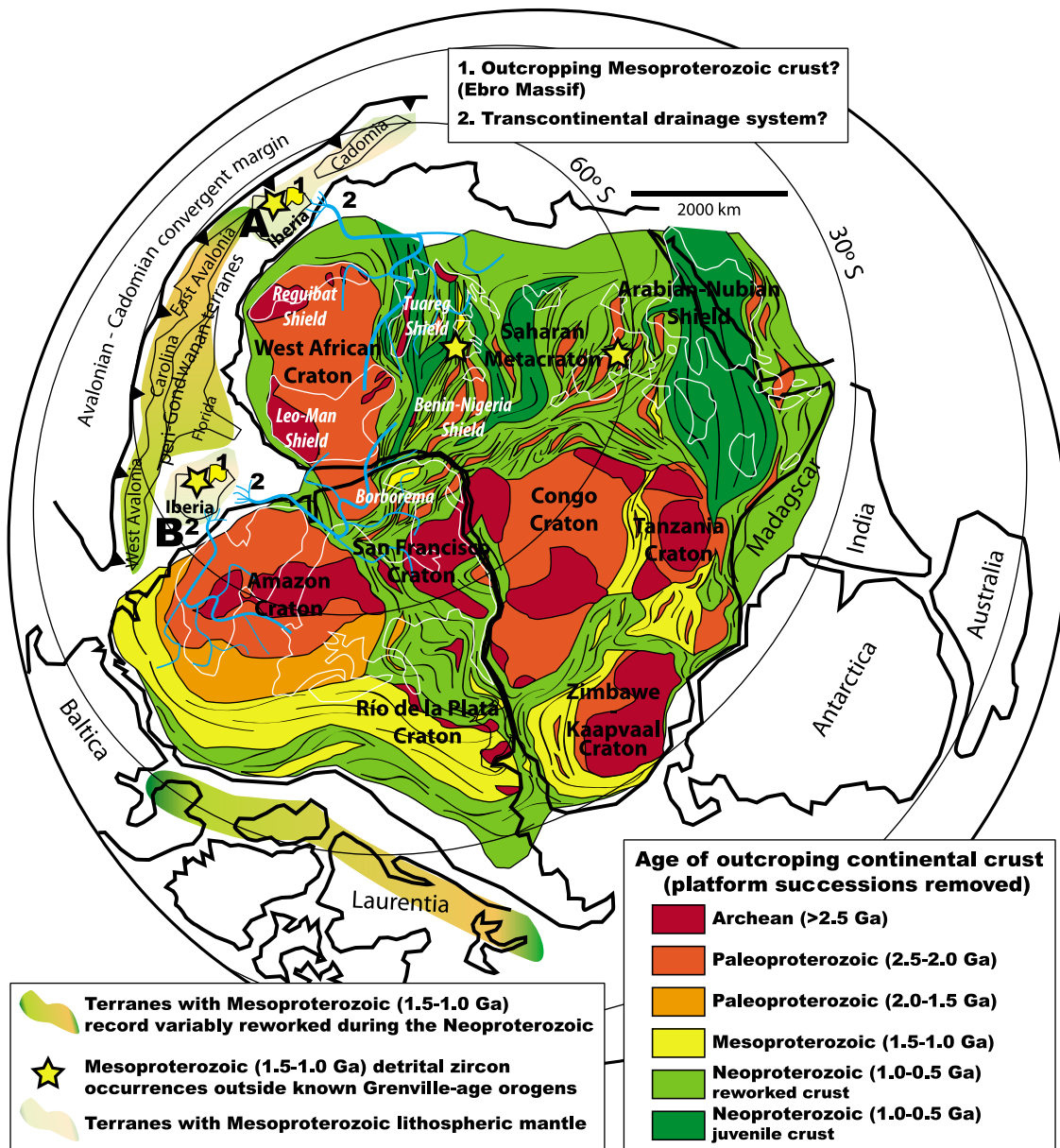


Figure 9. Neoproterozoic reconstruction of Gondwana presenting two paleopositions of Iberia (A and B) and providing in each case two explanations (labels 1 and 2, explained in the top inset) for the occurrence of Mesoproterozoic detrital zircons in Iberia. The two alternative paleopositions of Iberia shown share a similar paleolatitude. A is north of the West African Craton [e.g., after *Linnemann et al.*, 2008, 2011], whereas B is adjacent to both the West African and Amazon Cratons [e.g., after *Gutiérrez-Alonso et al.*, 2005; *Nance et al.*, 2008; *Murphy et al.*, 2009]. Supercontinental organization comprises near-surface or outcropping Archean s.l. nuclei surrounded or reworked by Paleoproterozoic, Mesoproterozoic and Neoproterozoic orogenic belts. Many areas are currently covered by platform successions not shown in this reconstruction (ranging from Mesoproterozoic to Mesozoic-Tertiary age). Neoproterozoic platforms may exhibit lateral connections with coeval orogenic belts or tectonic zones of the so-called Pan-African, Trans-Saharan or Trans-Brasiliano megasuture. Thin white lines represent current outcrop boundaries of various principal cratons. In addition to the references already cited above, the reconstruction is based upon compilations of *Unrug* [1997], *Murphy et al.* [2006, 2008, 2009], *Linnemann et al.* [2008, 2011] and references therein. See text for further details.

penetratively deformed (and admittedly Ediacaran) Anguiano schists.

5.2. Interpretation of Archean, Paleoproterozoic and Mesoproterozoic Ages

[32] We interpret the oldest age groups found as representing juvenile orogenic magmatism involved in continental collisions and formation of interior orogens during the closing stages of a supercontinental cycle. Neoproterozoic zircons (2.56–2.52 Ga) can be tentatively attributed to the continental assemblies of Superia and Sclavia [Bradley, 2011], whereas Paleoproterozoic zircons (2.27–1.70 Ga) would relate to later collisions of the fragments resultant from Neoproterozoic supercraton breakup. In fact, the Paleoproterozoic Orosirian period (from “orosira,” mountain range), which lasted from 2.05 to 1.80 Ga, is regarded as a global orogenic period on virtually all continents, notably between 1.90 and 1.85 Ga [cf. Robb et al., 2004]. The supercontinent Nuna amalgamated at this time [Bradley, 2011; Evans and Mitchel, 2011].

[33] Early Mesoproterozoic (1.54–1.47 Ga) zircon ages actually encompass the late Paleoproterozoic and early Mesoproterozoic. Spots of this group provided a few concordant and mostly discordant ages related to the Paleoproterozoic Statherian period (from “statheros,” stable, which lasted from 1.8 to 1.6 Ga) and the Mesoproterozoic Calymnian period (1.6–1.4 Ga, from “calymma,” cover). Both periods are related in most continents to final cratonization of earlier fold belts or to the development of platforms. We interpret that this age group might represent anorogenic reworking or partial remobilization of older crust. By contrast, middle to late Mesoproterozoic zircons are here interpreted as representative of orogenic magmatism related to Rodinia supercontinental assembly around 1.0 Ga ago [Weil et al., 1998]. In fact, narrow metamorphic belts characterize the 1.2–1.0 Ga period (called Stenian after “stenos,” narrow) and have been usually related to continental interactions.

[34] The Neoproterozoic Tonian (after “tonas,” stretch) and Cryogenian (after “Cryos,” ice, and “genesis,” birth) zircon age groups are interpreted to reflect the reworking of older crust during the onset of a new supercontinental cycle after amalgamation of Rodinia [Unrug, 1997; Bradley, 2011]. Late Neoproterozoic (Ediacaran) ages are here interpreted as reflecting the magmatic origin of zircons associated to the formation of late Neoproterozoic juvenile crust. The tectonic setting for this magmatism in the Iberian Peninsula related to magmatic arcs and back-arc basins [e.g., Ugidos et al., 1997; Fernández-Suárez et al., 1998; Eguiluz et al., 2000] associated to peri-Gondwanan orogens.

5.3. Neoproterozoic Zircon Provenance

[35] Following Quesada's [1990] paleotectonic reconstruction of the Cadomian (late Neoproterozoic-early Cambrian) Iberian orogen, the location of the area occupied by the current Sierra de la Demanda was within the Iberian autochthon (as an emerged land) or at its continental margin (then being part of a marine sedimentary basin). The (emerged) source region for the late Neoproterozoic sedimentary successions in this and the neighboring areas (central and northern Iberia) was extensive and thoroughly homogenized [Ugidos et al., 2010]. The magmatic origin of most zircons of Neoproterozoic age analyzed in this study

(e.g., Figures 4a, 4b, 4d, and 4e) can be related to magmatic arc and back-arc basin tectonic settings (Figure 9) related to a peripheral orogen [e.g., Ugidos et al., 1997; Fernández-Suárez et al., 1998]. Relics of this arc system are preserved in the Ossa-Morena Zone of the southern Iberian Massif, where outcrops of Neoproterozoic metamorphic rocks intruded by Cadomian plutons or unconformably covered by thick volcanosedimentary complexes abound [Eguiluz et al., 2000; Bandrés et al., 2002, 2004, and references therein]. Currently, lateral equivalents of this arc (in comparable paleotectonic positions and currently close locations) are thought to crop out in the western Anti-Atlas Neoproterozoic inliers [Thomas et al., 2004] and in the Armorican Massif [Chantraine et al., 2001].

[36] The Neoproterozoic sedimentary basin itself formed part of the northern Gondwanan paleotectonic realm, within the so-called Avalonian-Cadomian convergent margin [Unrug, 1996]. The magmatic arc was built close to the site of lithospheric convergence (the active margin), whereas the Neoproterozoic back-arc ocean would separate it from mainland Gondwana (Figure 9). This arc was likely adjacent to a marginal sea that was the actual site of the Neoproterozoic basin, filled by detritus carried from the continental and arc sides. Its sedimentary fill had, thus, a double origin: the magmatic arc itself to the North (in current geographical coordinates) and the continental mass of Neoproterozoic Gondwana to the South. The latter would have likely developed a passive continental margin fed by transcontinental river systems.

[37] A current analogue of this paleogeographic setting exists in eastern Asia, where the Yellow, Yangtze, Pearl, Red or Mekong Rivers discharge in the Japan, Yellow and China Seas, which are separated from the main Pacific Ocean by magmatic arcs. Some published zircon provenance studies relate to fluvial basins such as these (e.g., the Yellow or Amazon rivers) [cf. Mapes et al., 2004]. In these current examples, transcontinental rivers drain geologically complex continental basins (with remnants of older orogens, platforms and cratons) several thousands to millions of square km in area. The example of the paleo-Lena River [Prokopyev et al., 2008] shows that fluvial systems such as these can be active during several tens to hundreds of Myr. Lawrence et al. [2010] have shown that detrital zircon hydrodynamic fractionation in a sedimentary basin can induce zircon population variations (even missing of some age populations), since zircons track with hydraulically comparable detrital grains. Similarly, Linnemann et al. [2011] have demonstrated that in current northern Africa (north Gondwana) detritus of the widespread Neoproterozoic-early Paleozoic platform sequences were actually derived from different cratons and terranes.

5.4. Archean, Paleoproterozoic and Mesoproterozoic Zircon Provenance

[38] The Archean and Proterozoic continental basement eroded and sampled by the Iberian Ediacaran sedimentary basin does not outcrop currently and very little is known on its lithological nature, though it is widely accepted that it formed part of Gondwana [e.g., Linnemann et al., 2008] and that it was related to North-West Africa [Quesada et al., 1991; Murphy et al., 2004] or, maybe, South-American [Fernández-Suárez et al., 2000; Zeck et al., 2004; Gutiérrez-

Alonso *et al.*, 2005] or North-Eastern African [Díez Fernández *et al.*, 2010] counterparts (see Figure 9). This dicotomy was originated in relation with the paleotectonic setting of Neoproterozoic Newfoundland [Murphy *et al.*, 2002; Mac Niocaill *et al.*, 2002]. It has been put into discussion in Iberia, too, even for epochs more recent than the Neoproterozoic. For example, Cocks and Torsvik [2002] located the Iberian autochthon during the Ordovician in a position close to northwest Africa, based upon faunal and paleomagnetic constraints. By contrast, Gutiérrez-Marco *et al.* [2002] located Iberia near central-eastern Africa, close to Algeria or Libya, based upon paleontological correlations of benthic faunas at the species level. Finally, Bea *et al.* [2010] located Iberia farther East, adjacent to the Arabian-Nubian shield, on the basis of their similar zircon geochronology and Nd isotope signatures. Complementary to this, Morag *et al.* [2011a, 2011b] and Avigad *et al.* [2012] suggested (based upon a significant amount of Tonian and Stenian detrital zircon ages from Cambrian sandstones) that parts of southwestern Europe might have been connected to shield sources located in central and eastern domains of North Africa.

[39] The Gondwanan mainland around current Iberia is formed by a number of cratons (Amazonian in South America and West African, Saharan and Arabian-Nubian in North Africa) that are themselves composite pieces made of older cratons, orogens, and mildly deformed platforms, ranging in age from the Archean to the Neoproterozoic (Figure 9). The surface geology of these continental masses [e.g., Choubert and Faure-Muret, 1990; Schobbenhaus and Bellizia, 2001] consists in most cases of Archean nuclei surrounded or reworked by Paleoproterozoic and younger orogenic belts, and covered by platform successions of various ages. Neoproterozoic platform deposits cover unconformably older cratonic masses and sometimes exhibit lateral connections with either Neoproterozoic orogenic belts surrounding older cratons or with tectonic zones suturing them. These orogens collectively build a major interior orogen active between 850 and 530 Ma (the so-called Pan-African, Trans-Saharan or Trans-Brasiliano megasuture).

[40] Craton geochronological signatures have been recognized notably through zircon provenance studies and radiometric datings [e.g., Abdelsalam *et al.*, 2002; Ali *et al.*, 2009; Horton *et al.*, 2010]. These and many other papers have highlighted that the West-African craton lacks the fingerprint of orogenic activity related to amalgamation of Rodinia around 1.0–1.2 Ga ago [Weil *et al.*, 1998], in contrast with some neighboring cratonic masses, particularly the Amazonian, Saharan and Arabian-Nubian shields, which preserve such record. This also applies partly to the so-called Cadomian terranes of West Europe, in contrast to Avalonian ones. Though both occupied a marginal position in North Gondwana during the Neoproterozoic, the former are characterized by a lack of Mesoproterozoic magmatism, whereas in the latter a major content of Mesoproterozoic relics is observed [Murphy *et al.*, 2004]. These general assumptions, however, can be examined in more detail and sometimes discussed, as shown in the following review.

[41] Johnson and Woldenhaimanot [2003] and Kröner and Stern [2005, and references therein] showed that the Arabian-Nubian shield of NE Africa consists of a few continental fragments with Archean and Paleoproterozoic rocks

and that Pan-African amalgamation of cratons and orogens, including magmatic terranes that begun to form at ca. 870 Ma, was completed by 600 Ma. Ali *et al.* [2009] showed that juvenile Neoproterozoic igneous and sedimentary rocks dominate the surface geology of this region and that pre-Neoproterozoic xenocrystic zircons (of Neoproterozoic, Paleoproterozoic and late Mesoproterozoic age groups) are common in them. Though no major outcrops of Mesoproterozoic (ca. 1.0–1.3 Ga) rocks exist currently, continental crust of this age was involved in the genesis of Neoproterozoic rocks, due to either the magmatic recycling of subsurface continental crust occurrences, the erosion elsewhere and transportation of detritus to the Neoproterozoic deposition sites, or by its subduction-related reworking.

[42] Abdelsalam *et al.* [2002] coined the term “Saharan metacraton” to refer to the pre-Neoproterozoic continental crust that was highly remobilized during the Neoproterozoic in the north-central part of Africa. In a revision of its geological, geochronological and isotopic characteristics, its boundaries, lithology and structure, these authors described a medium- to high-grade metamorphic remobilization during the Neoproterozoic (750–550 Ma) of Neoproterozoic (3.10–2.45 Ga), Paleoproterozoic (2.30–1.60 Ga) and Mesoproterozoic crust (1.23–0.90 Ga), likely reflecting several episodes of juvenile crust formation and/or reworking of older crust. Mesoproterozoic crust remobilization has been unraveled notably in the eastern boundary of the metacraton [Küster *et al.*, 2008].

[43] The Neoproterozoic trans-Saharan belt sutured the Saharan metacraton and the West African craton. It crops out in the Tuareg and Benin-Nigeria Shields, and extends to the south into the trans-Brasiliano belt (Figure 9). In the early Paleozoic platform sequences overstepping the trans-Saharan belt, Linnemann *et al.* [2011] recovered 1.30–1.80 Ga detrital zircons. According to these authors (and references therein), sources to these Meso- to late Paleoproterozoic relics are unknown in the West African craton, but have been reported in the eastern Saharan Metacraton and also in the Tuareg Shield, where have been interpreted as records of protolith ages of pan-African orthogneisses, of granite cobbles included in Neoproterozoic successions, and of the igneous precursors of pan-African recycled granitoids. In spite of this evidence, direct proof of outcropping Mesoproterozoic crust is missing in the trans-Saharan belt, the nearest occurrences being the Saharan metacraton and the Amazonian craton.

[44] Cordani and Teixeira [2007] showed that in the Amazonian craton a Paleoproterozoic nucleus (made of Archean crust, Paleoproterozoic supracrustals and granitoids) grew by accretion of younger orogenic belts (soft-collisions) during three successive tectonic cycles dated 2.0–1.8, 1.78–1.55 and 1.5–1.3 Ga. This cratonic ensemble collided 1350–1000 Ma ago with Laurentia forming a Mesoproterozoic (“Grenville” age) orogenic belt. This was followed by anorogenic magmatism dated 1000–970 Ma and then by a new supercontinental cycle that, after 200 Myr of ocean basin consumption and calc-alkaline magmatism, concluded with the formation of the Brasiliano orogen in the 700–500 Ma interval (related to amalgamation of Gondwana). This geological evolution is currently recorded by a series of Paleoproterozoic and Mesoproterozoic tectonic provinces progressively younger to the West (in current geographical coordinates) cut across by the Brasiliano belt to the southeast [Chew *et al.*,

2007]. Notwithstanding, occurrence of Mesoproterozoic reworked crust has been reported, too, in the Borborema area of NE Brazil [cf. *Linnemann et al.*, 2011] (Figure 9), close to coeval occurrences of western Africa described below.

[45] The West African craton crops out in various massifs made of Archean (3.5–3.0 Ga and 2.95–2.75 Ga) and Paleoproterozoic (2.2–1.75 Ga) nuclei and Neoproterozoic orogenic belts (see recent reviews of *Abati et al.* [2010, and references therein] and *Linnemann et al.* [2011, and references therein]). The Paleoproterozoic orogens record medium- to high-grade metamorphism attributed to the so-called Eburnian-Birimian orogeny (prior to 1.76 Ga). They are covered unconformably by Neoproterozoic platform sedimentary successions. The Neoproterozoic orogens (cropping in the Anti-Atlas inliers, as well as in the Tuareg and the Benin-Nigeria shields) exhibit clear tectonic and geometrical connections with coeval counterparts of north-east Brazil and are unconformably covered by late Neoproterozoic to Paleozoic sedimentary rocks. A depositional lack in the 1.7–1.0 Ga interval [*Clauer et al.*, 1982] has been acknowledged as a characteristic feature of the West African craton. This is remarkable, since Mesoproterozoic sediments cover the other Gondwanan cratons and complements the apparent absence of any remnant of Mesoproterozoic tectono-magmatic events. Recent geochronological studies, however, have shown that sedimentary successions regarded as early Neoproterozoic (and delimited by regional unconformities) are actually Mesoproterozoic (1.1 Ga) [cf. *Rooney et al.*, 2010], and provide connections between the geodynamic evolution of this craton and that of others involved in the formation of the supercontinent Rodinia. In particular, *Tohver et al.* [2006] supported with paleomagnetic data a Mesoproterozoic suture (“Grenvillian”) between Laurentia and the juxtaposed Amazonian and West African cratons. They also showed that the Arabian-Nubian craton has a contrasting paleomagnetic drift history that suggests that it was not a part of Rodinia, though it was assembled with Amazonia-West Africa and other Gondwanan cratons during Neoproterozoic times.

5.5. Cambrian Cobble and Detrital Zircon Provenance

[46] Pre-Cambrian relics preserved in Iberian sedimentary rocks might have been derived from any of the Proterozoic constituents referred to above (depending upon its Neoproterozoic to early Cambrian position) or, more likely, from closer, concealed Iberian equivalents. In addition to well known recycled detrital zircon grains, Proterozoic or older relics also include igneous and metamorphic pebbles of earliest Cambrian conglomerate layers [*Colchen*, 1974; *Álvaro and Vennin*, 1998; *Liñán et al.*, 2002; *Álvaro et al.*, 2008; *Rubio-Ordóñez*, 2010; *Ábalos et al.*, 2011] and granulite-facies rock samples recovered from deep submarine exploration in the Bay of Biscay continental margins [*Capdevila et al.*, 1974; *Guerrot et al.*, 1989; *Gardien et al.*, 2000, and references therein].

[47] The Anguiano quartz-pebble conglomerate lithotype is thought to register specific paleoclimatic or paleogeographic characteristics: tectonically quiescent conditions under which weathering (chemical and mechanical) was very efficient and included prolonged mechanical abrasion, intense chemical weathering or older conglomerate recycling [cf. *Cox et al.*, 2002]. The lithological and accessory mineral

evidence preserved (Figure 4) suggests that magmatic, low- to high-grade metamorphic and sedimentary rocks cropped out in the conglomerate source area. The geometry, dimensions, sedimentary environment and current tectonic setting (due to Alpine tectonism) deduced for this formation make it reasonable to expect that the outcrops of those source rocks should not occur too far (a few tens of km) from the conglomerate deposition site, within Iberia. Source region candidates in present-day Iberia are: (1) the outcropping Neoproterozoic domains of the Iberian Massif (located toward the West), (2) the poorly known mid- and lower crustal segments of the Iberian microplate continental margin [*Guerrot et al.*, 1989; *Gardien et al.*, 2000] and (3) the concealed “Ebro Massif” (located toward the East) of the Iberian regional literature, currently hindered under a km-thick Mesozoic to Tertiary cover.

[48] Concerning the first case, Neoproterozoic rocks currently exposed in the central and northwestern Iberian massif were not subjected to metamorphism higher than low-grade. Additionally, these rocks bear vestiges that place them close to a magmatic arc, such as subvolcanic intrusives, magmatic rock cobbles, or their inherited geochemical features [e.g., *Fernández-Suárez et al.*, 1998, 2000; *Ugidos et al.*, 1997, 2010; *Rubio-Ordóñez*, 2010]. Low- to high grade Neoproterozoic metamorphic rocks showing high-temperature crystal-plastic quartz deformation are only known to occur in the Ossa-Morena Zone [*Ábalos*, 1992] of the southern Iberian Massif. The Neoproterozoic to Cambrian magmatic arc setting is more evident here than in the central and northern segments of the Iberian Massif. The Ossa-Morena zone was accreted to the Iberian autochthon during the Cadomian orogeny [*Quesada*, 1990; *Ábalos*, 1992]. However, this accretion and some of its syn- to post-tectonic magmatic intrusions are roughly coeval to younger than the early Cambrian successions of the Sierra de la Demanda, thus precluding this or a lateral equivalent as a source region.

[49] As regards mid- and lower crustal segments of the Iberian microplate (exposed in the Atlantic seafloor of the continental margin of Iberia [cf. *Capdevila and Mougenot*, 1988]), these might be good candidates as sources for the metamorphic pebbles. Some Neoproterozoic to Paleoproterozoic recovered metamorphic rocks [*Guerrot et al.*, 1989] were already exhumed in the Mesoproterozoic [*Gardien et al.*, 2000], perhaps implying that some kind of tectonic activity (enabling mid- to lower crustal exhumation) was recorded by the Mesoproterozoic Iberia. Mesoproterozoic, supra-subduction zone ophiolite relics discovered by *Sánchez-Martínez et al.* [2006] led these authors to suggest that, likely, such tectonism was not related directly to the Grenville orogen, but might have correspond to obduction of a peri-arc oceanic lithosphere over the paleocontinental margin of West Africa during the assembly of Rodinia 1.1–1.0 Ga ago. Later, *Sánchez-Martínez et al.* [2011] disregarded such a hypothesis and interpreted this zircon population as resulting from the involvement of a North Gondwanan Mesoproterozoic basement in late Paleozoic magma generation. *Villaseca et al.* [2011] identified, too, the involvement of pieces of a Mesoproterozoic crustal basement (1.0–1.2 Ga) in the autochthon of central Iberia. The current location of these units, hundreds of km away from the early Cambrian conglomerates that contain the metamorphic pebbles, are at odds with the hypothesis that they

are direct source regions. Notwithstanding, the possibility exists that currently concealed equivalents made of similar mid- to lower crustal materials exist near the Sierra de la Demanda. So far, these would occur buried under the variably thick Paleozoic and Mesozoic-Tertiary successions but during the late Neoproterozoic-early Cambrian they likely cropped out forming the “Ebro Massif.” To our knowledge, the Ebro Massif has never been drilled, but its existence is supported by stratigraphic source regions studies of terrigenous Mesozoic successions exposed in the Iberian Ranges and parts of the Basque Cantabrian Basin. *Murphy et al.* [2008] have shown that Ordovician magmatic rocks from northwest Iberia probed a concealed basement such as this. Subidiomorphic detrital zircons of that age such as the 1341 ± 26 Ma old one shown in the Figure 4d demonstrate that outcropping Mesoproterozoic magmatic rocks were eroded and transported not too far before incorporation to the Anguiano Conglomerate in the earliest Cambrian.

5.6. Tectonic Constraints Provided by the Iberian Subcontinental Mantle

[50] Sm-Nd isotopic studies trace the origin of outcropping Iberian basement rocks (Neoproterozoic to pre-Permian) to a geochemical heterogeneous subcontinental mantle enriched during the late Mesoproterozoic, as model ages for most Neoproterozoic-Paleozoic Iberian rocks usually range from 1.0 to 1.6 Ga [*Nägler*, 1990; *Nägler et al.*, 1992, 1995; *Murphy et al.*, 2008; *Bea et al.*, 2010; *Fernández-Suárez et al.*, 2011, and references therein]. Evidence for the involvement of Mesoproterozoic crustal and subcontinental mantle is widespread for the Ordovician magmatism of northwest Iberia as well as for the Cadomian (Neoproterozoic-Cambrian) metaigneous basement across the Iberian Massif. Complementary to this, *Guerrot et al.* [1989] pointed out that Nd model ages of Archean and Paleoproterozoic zircons from granulites dredged in the north Iberian continental margin (sampling the Iberian lower crust?) are older than their U-Pb ages. All these isotopic data support some kind of relationship between crustal and mantle rocks in relation to orogenesis either during Archean/Paleoproterozoic times (which is admitted in the bibliography), or during the Mesoproterozoic (currently under debate).

[51] During orogenesis the lithospheric mantle acquires penetrative fabrics (due to lattice-preferred orientation of peridotite minerals) that are frozen at the end of tectonism as it cools below a critical blocking temperature (800–900°C) so that olivine creep becomes ineffective over geologically significant time scales. These fabrics are correlated in most orogens with the trends and kinematics of crustal surface structures, thus providing a basis to gathering information though seismic anisotropy studies of the upper mantle that can be used to decipher its frozen structural grain [e.g., *Vaucher and Nicolas*, 1991; *Vaucher and Barruol*, 1996].

[52] Resetting of the Sm-Nd signature of the subcontinental lithospheric mantle, from which most igneous and sedimentary rocks are actually derived, is possible through thermal erosion, partial melting and diapirism. Temperatures required to achieve this are of 1200–1300°C, barely the isotherm used to separate the base of the lithosphere and the asthenosphere, where rock fabric development is related to active mantle flow. In outcropping mantle rocks this is manifested by recrystallization fronts separating coarse-

granular peridotites partially molten under asthenospheric P-T conditions (above 1200°C and 1.5 GPa) and porphyroclastic peridotites deformed in the solid state under lithospheric (800–1000°C) high-grade P-T conditions [e.g., *Vaucher and Garrido*, 2001; *Tubía et al.*, 2004, and references therein]. *Van der Wal and Bodinier* [1996] and *Garrido and Bodinier* [1999] showed that asthenospheric recrystallization fronts can retain the lattice preferred orientations of the pre-existing subcontinental lithospheric mantle and that, though the recrystallized peridotites do not represent a genuine asthenosphere, their chemical and isotopic composition varies sharply from that of the lithospheric peridotite precursors.

[53] The ILIHA (Iberian Lithospheric Heterogeneity and Anisotropy) large-scale deep seismic sounding experiment [*ILIHA DSS Group*, 1993] provided a first image of the lateral heterogeneity of the lithospheric mantle beneath the western Iberian Peninsula, which remained stable for the last 300 Ma. *Ábalos and Díaz-Cusí* [1995] postulated a correlation with the major structures and tectonic history of the outcropping basement rocks in SW Iberia though a model of polyorogenic lithosphere deformation. It was characterized by a subcontinental mantle heterogeneity defined by Variscan lithospheric shear zones inducing major thermal effects in the crust and separating pre-Variscan (arguably Cadomian, or older) subcontinental mantle pieces with contrasting fabrics. *Vaucher and Barruol* [1996], *Barruol et al.* [1998], and *Souriau et al.* [2008, and references therein] completed this image for the Pyrenean realm of Iberia and evidenced there that upper mantle anisotropy correlates with surface structures and is related to frozen (Tertiary/Alpine and pre-Mesozoic/Variscan) lithospheric structures.

[54] *Fernández-Suárez et al.* [2011] suggested that the primordial origin of the Iberian lower crust is often 0.9–1.2 Ga and argued that the rare pre-Cadomian zircons had been consumed in earlier stages of melting in the lower crust, while the Sm-Nd rock signature was retained. The differences between the common Cadomian U-Pb datings and Mesoproterozoic Sm-Nd model ages are explained this way through the opening of the isotopic systems during high-grade tectonothermal events, crustal recycling or the choice of a depleted mantle reservoir model. *Gutiérrez-Alonso et al.* [2011] observed contrasting Sm-Nd isotopic signatures between pre- and post-middle Permian mantle-derived mafic rocks interpreted as due to another tectonothermal resetting, now due to the replacement (delamination) of part of the Iberian subcontinental lithospheric mantle during Carboniferous-Permian oroclinal bending. These features differ from those of the relics of the subcontinental mantle cropping out in the Allochthonous Complexes of NW Iberia. *Santos et al.* [2002], *Pin et al.* [2006], and *Murphy and Gutiérrez-Alonso* [2008] have shown that those relics bear Gondwanan affinities, reflect juvenile mantle development 500 Ma ago in a suprasubduction zone setting, are closely related to the Rheic Ocean, and were thrust upon Gondwana during ocean closure.

[55] All the above discussion permits us to suggest that, likely, the Iberian subcontinental lithospheric mantle was originated (reset after an earlier precursor?) in the Mesoproterozoic, right after some major orogenic episode. Complementary to this, coeval juvenile and reworked crust might have been captured during continental collisions leading to

supercontinent formation and preserved since that time [Condie *et al.*, 2011]. Maybe the crustal surface expression of these processes cropped out during the Neoproterozoic, though currently has been largely erased or is concealed under a Phanerozoic cover. Subsequently, the subcontinental mantle underwent generalized orogenic deformation under lithospheric conditions during the Neoproterozoic (Cado-mian orogeny), as well as localized deformation under comparable conditions during the late Paleozoic (Variscan orogeny) and the Tertiary (Alpine orogeny). Given that any of these lithospheric realms had been delaminated, and the subcontinental mantle asthenospherized (e.g., as proposed by Blanco and Spakman [1993] or Gutiérrez-Alonso *et al.* [2011]), the previous mantle fabrics would not have been retained so as to be currently detectable through seismic anisotropy subcontinental sounding.

5.7. Paleotectonic Setting

[56] We hypothesize, following Gutiérrez-Alonso *et al.* [2005], Murphy *et al.* [2008], or Villaseca *et al.* [2011] that Mesoproterozoic lithosphere relics exist (or might have existed prior to 300 Ma ago [cf. Gutiérrez-Alonso *et al.*, 2011]) in the concealed basement of Iberia (the core of the Ibero-Armorican Arc) and that tracts of continental crust with similar characteristics crop out currently in the Precambrian cratons of Northwest Africa (Tuareg Shield) and South America (Borborema province; see Figure 9). As geological knowledge of the north-Gondwanan cratons improves, evidence for the existence of widespread Mesoproterozoic tectono-magmatic or tectono-sedimentary activity is clearer [e.g., Linnemann *et al.*, 2011; Avigad *et al.*, 2012]. As discussed in a preceding section, Mesoproterozoic metamorphic rocks are known in the Amazonian craton, in the Trans-Saharan belt, and along the boundary between the Arabian-Nubian shield and the Saharan metacraton (Figure 9). In the Iberian Peninsula relics of these groups have been identified, too. Sedimentary rocks carrying inherited Mesoproterozoic zircons are known so far in all these continental pieces, and these might be the sources of recycled detrital zircon grains or of sandstones carrying detrital zircons like those already recognized in NW Iberia [Fernández-Suárez *et al.*, 2000; Zeck *et al.*, 2004; Gutiérrez-Alonso *et al.*, 2005] or analyzed in this study. Additionally, if a large continental river system was associated to the Neoproterozoic paleogeography, detrital zircon hydrodynamic fractionation [Lawrence *et al.*, 2010] could have occurred, inducing zircon population variations (even missing of some age groups).

[57] It has been suggested that the Iberian paleo-Massif occupied a Neoproterozoic position between the West African and the Amazonian cratons [e.g., Gutiérrez-Alonso *et al.*, 2005; Nance *et al.*, 2008; Murphy *et al.*, 2009], a few thousands of km apart along the Avalonian-Cadomian convergent margin but still close to the West African craton [e.g., Díez Fernández *et al.*, 2010; Linnemann *et al.*, 2011] (see both possibilities in Figure 9). Alternatively, other studies either suggest or would favor a position closer to the Arabian-Nubian shield [Bea *et al.*, 2010; Díez Fernández *et al.*, 2010; Morag *et al.*, 2011a, 2011b]. Complementary tectonic hypotheses have been invoked to explain the movement of Iberia to its well known late Paleozoic position. At the same time, some already available data

may have been disregarded depending on its adjustment to those models.

[58] Díez Fernández *et al.* [2010] argued that no late Neoproterozoic suture or dextral megashears affecting the rim of northern Gondwana have been identified so far, neither in Iberia nor in the European Variscides, thus impeding the approximation of Amazonia-derived terrains to north Africa. However, the occurrence of a late-Neoproterozoic to early Cambrian suture has long been described in SW Iberia [after Quesada, 1990] and has been characterized taking into account independent, geological and geophysical data sources [Ábalos, 1992; Ábalos and Díaz-Cusi, 1995] that highlight the importance of dextral orogen parallel displacements at the time. Paleosutures are known to be prone to orogenic reactivation [Vauchez and Nicolas, 1991; Vauchez *et al.*, 1997]. Additionally, as sutures represent the blocking sites of paleosubduction zones and protracted tectonic erosion is capable (at a geological time scale) of removing large tracts of continental crust and recycle them into the mantle (as proposed by Scholl and Von Huene [2007]), the conjunction of all this can explain that older suture relics (for example Mesoproterozoic), when still present, occur as strongly reworked and difficult to unravel tectonic pieces forming part of younger continental suture zones (Figure 9). In spite of this, their isotopic fingerprints are preserved in the lithospheric mantle and the igneous rocks originated after it.

[59] From a complementary perspective, the well-constrained paleotectonic reconstructions of the Variscan orogen in the North Atlantic realm [e.g., Matte, 1991; Michard *et al.*, 2010] locate the Iberian Massif 300 Ma ago adjacent to northwest Africa (between the Gibraltar strait and Tunisia), separated by a major dextral transcurrent fault. This fault enables accommodation of orogenic bends induced by the East facing Newfoundland/Grand Banks promontory and the West facing Ibero-Armorican one. The drifting of Iberia from East Africa locations 450 Ma ago (as suggested by Bea *et al.* [2010] to the 300 Ma paleoposition cited above would require the drift along a transform or transcurrent fault at moderate to slow rates (1–3 cm/yr during a 150 Myr interval) that might explain the differences in the Paleozoic stratigraphy of Variscan Iberia and Morocco. Such a transcurrent movement zone should have played mostly as sinistral during the Iberian drift, which contrasts with its dextral character during the final stages of continental collision. We envisage this is not incompatible, neither impossible. It is possible that Iberia remained adjacent to northeast Africa during the 200–300 Myr period between the Cryogenian or Early Ediacaran and the Ordovician, but this is not supported by recent paleomagnetism.

[60] Paleomagnetic and paleogeographic reconstructions of North Gondwana [Courjault-Radé *et al.*, 1992; Debrenne and Courjault-Radé, 1994; McCausland *et al.*, 2006] locate Iberia during the late Ediacaran and early Cambrian in a position comparable to that described above for Latest Carboniferous times (300 Ma ago). Iberia forms part of the Avalonian-Cadomian terranes in these reconstructions, building the peri-Gondwanan active margin (Figure 9). Iberian-Moroccan and Iberian-Avalonian connections are often proposed on the basis of paleontological and stratigraphic correlations [Babcock *et al.*, 2005]. Thompson *et al.* [2007] have shown that paleomagnetic studies that locate Avalonia 600 Ma ago at a paleolatitude of 38° are

compatible with its position either adjacent to the West African Craton (38°S) or adjacent to the western Amazonian Craton (38°N). In both cases Avalonia would be situated along the active margin of north Gondwana. This is compatible, too, with the paleomagnetic data of *Tohver et al.* [2006], which suggest that both cratons formed a unique mass that first collided with Laurentia during the Mesoproterozoic, welded by a Grenvillian suture, and then (during the middle Cambrian) collided with the other central- and Nord-Gondwanan cratons, forming the trans-Brasiliano megasuture. If these hypotheses were true, the Mesoproterozoic signature of Iberia could have been originated in a Meso- and Neoproterozoic West African or Amazonian craton connection. From these two possibilities, in our view, the West African connection north of the Reguibat shield (possibility A in the Figure 9) would explain better the general scarcity of Mesoproterozoic zircon relics than ubication of Iberia at the same latitude but closer to the Amazonian craton (possibility B in the Figure 9). A third viable possibility would position Iberia north of the Tuareg and the Arabian-Nubian shields [Avigad *et al.*, 2012].

6. Conclusions

[61] Early Cambrian conglomerates from the Sierra de la Demanda contain metamorphic and sandstone pebbles with detrital zircons. U/Pb zircon dating permits us to constrain the maximum depositional age of the azoic, early Cambrian sechron and to contribute with additional data to the ongoing discussion on Iberian zircon provenance and paleotectonic reconstructions that relate Iberia with Amazonian, West African or East African cratonic counterparts.

[62] We identify Paleoproterozoic, Mesoproterozoic and Neoproterozoic zircon populations and discuss their likely origin in the context of the Avalonian-Cadomian Neoproterozoic active margin of Gondwana and the Paleoproterozoic (and older) relics of all Nord-Gondwanan cratons. The Mesoproterozoic age group was supposed to be absent in the West African craton and, subsequently, was used to relate Iberia with two possible paleopositions of Iberia separated a few thousands of km apart, either to the East (near the Arabian-Nubian craton) or to the West (near the Amazonian craton). The Iberia-Amazonia connection suggested by various authors has been rejected by more recent studies supporting a connection between Iberia and central-eastern North Africa. We show that (1) the paleotectonic criteria used to withdraw the first hypothesis are imprecise, (2) recently published studies provide geological, geochemical and geochronological evidence on the existence of a Mesoproterozoic geodynamic record also in the West African Craton as well as in Iberia, and that (3) recent paleomagnetism studies show that Amazonia and West Africa formed a unique mass which during the Mesoproterozoic collided with another continent along a Grenvillian suture. We explain the loss of most relics of this suture in West Africa by orogenic reactivation and subduction erosion. Recent paleomagnetic studies also show that during the middle Cambrian Amazonia-West Africa was sutured by the trans-Brasiliano megasuture with the other central- and Nord-Gondwanan cratons. This would have impeded a late Ediacaran to early Cambrian connection between Iberia and the Saharan metacraton or the Nubian-

Arabian shield, favoring a West-African-Amazonian relationship at that time. We argue that the basement of the Iberian Peninsula under the Paleozoic and Mesozoic covers of the Iberian Ranges might contain a Mesoproterozoic record and that it was an outcropping unit during the Ediacaran-Cambrian (the so-called Ebro Massif). In order to solve zircon provenance more accurately, future efforts should be directed, when possible, to dating the medium- to high-grade metamorphism recorded by early Cambrian conglomerate pebbles. So far, the lack of appropriate samples recovered for that purpose has permitted the question to remain highly speculative.

[63] **Acknowledgments.** We acknowledge the comments of J. J. Peucat, G. Zulauf, and two anonymous reviewers, which improved the quality of the original manuscript. Financial support was provided by the Spanish Ministerio de Ciencia e Innovación (Grupo Consolidado, project CGL2008-01130/BTE) and the Universidad del País Vasco (project GIU09/61).

References

- Ábalos, B. (1992), Variscan shear-zone deformation of late Precambrian basement in SW Iberia, implications for circum-Atlantic pre-Mesozoic tectonics, *J. Struct. Geol.*, *14*, 807–823, doi:10.1016/0191-8141(92)90042-U.
- Ábalos, B., and J. Díaz-Cusí (1995), Correlation between seismic anisotropy and major geological structures in SW Iberia: A case study on continental lithosphere deformation, *Tectonics*, *14*(4), 1021–1040, doi:10.1029/95TC01204.
- Ábalos, B., P. Puelles, S. Fernández-Armas, and F. Sarrionandia (2011), EBSD microfabric study of pre-Cambrian deformations recorded in quartz pebbles from the Sierra de la Demanda (N Spain), *J. Struct. Geol.*, *33*, 500–518, doi:10.1016/j.jsg.2011.01.005.
- Abati, J., A. Gerdes, J. Fernández-Suárez, R. Arenas, M. J. Whitehouse, and R. Díez-Fernández (2010), Magmatism and early Variscan continental subduction in the northern Gondwana margin recorded in zircons from the basal units of Galicia, NW Spain, *Geol. Soc. Am. Bull.*, *122*, 219–235, doi:10.1130/B26572.1.
- Abdelsalam, M. G., J.-P. Liégeois, and R. J. Stern (2002), The Saharan Metacraton, *J. Afr. Earth Sci.*, *34*, 119–136, doi:10.1016/S0899-5362(02)00013-1.
- Ali, K. A., R. J. Stern, W. I. Manton, J.-I. Kimura, and H. A. Khamees (2009), Geochemistry, Nd isotopes and U-Pb SHRIMP zircon dating of Neoproterozoic volcanic rocks from the Central Eastern Desert of Egypt: New insights into the ~750 Ma crust-forming event, *Precambrian Res.*, *171*, 1–22, doi:10.1016/j.precamres.2009.03.002.
- Álvaro, J. J., and E. Vennin (1998), Stratigraphic signature of a terminal Early Cambrian regressive event in the Iberian Peninsula, *Can. J. Earth Sci.*, *35*, 402–411, doi:10.1139/e97-093.
- Álvaro, J. J., B. Bauluz, A. Gil-Imaz, and J. L. Simón (2008), Multidisciplinary constraints on the Cadomian compression and early Cambrian extension in the Iberian Chains, NE Spain, *Tectonophysics*, *461*, 215–227, doi:10.1016/j.tecto.2008.04.006.
- Andersen, T. (2005), Detrital zircons as tracers of sedimentary provenance: Limiting conditions from statistics and numerical simulation, *Chem. Geol.*, *216*, 249–270, doi:10.1016/j.chemgeo.2004.11.013.
- Avigad, D., K. Kolodner, M. McWilliams, H. Persing, and T. Weissbrod (2003), Origin of Northern Gondwana Cambrian sandstone revealed by detrital zircon SHRIMP dating, *Geology*, *31*, 227–230, doi:10.1130/0091-7613(2003)031<0227:OONGCS>2.0.CO;2.
- Avigad, D., A. Gerdes, N. Morag, and T. Bechstädt (2012), Coupled U-Pb-Hf of detrital zircons of Cambrian sandstones from Morocco and Sardinia: Implications for provenance and Precambrian crustal evolution of North Africa, *Gondwana Res.*, *21*, 690–703, doi:10.1016/j.gr.2011.06.005.
- Babcock, L. E., and S. Peng (2007), Cambrian chronostratigraphy: Current state and future plans, *Palaeogeogr. Palaeoclimatol. Palaeoecol.*, *254*, 62–66, doi:10.1016/j.palaeo.2007.03.011.
- Babcock, L. E., S. Peng, G. Geyer, and J. H. Shergold (2005), Changing perspectives on Cambrian chronostratigraphy and progress toward subdivision of the Cambrian System, *Geosci. J.*, *9*, 101–106, doi:10.1007/BF02910572.
- Bandrés, A., L. Eguiluz, J. I. Gil Ibarguchi, and T. Palacios (2002), Geodynamic evolution of a Cadomian arc region: The northern Ossa-Morena

- zone, Iberian massif, *Tectonophysics*, 352, 105–120, doi:10.1016/S0040-1951(02)00191-9.
- Bandrés, A., L. Eguíluz, C. Pin, J. L. Paquette, B. Ordóñez, B. Le Fèvre, L. A. Ortega, and J. I. Gil Ibarra (2004), The northern Ossa-Morena Cadomian batholith (Iberian Massif): Magmatic arc origin and early evolution, *Int. J. Earth Sci.*, 93, 860–885, doi:10.1007/s00531-004-0423-6.
- Barrool, G., A. Souriau, A. Vauchez, J. Diaz, J. Gallart, J. Tubia, and J. Cuevas (1998), Lithospheric anisotropy beneath the Pyrenees from shear wave splitting, *J. Geophys. Res.*, 103, 30,039–30,053, doi:10.1029/98JB02790.
- Bea, F., P. Montero, C. Talavera, M. Abu Anbar, J. H. Scarrow, J. F. Molina, and J. A. Montero (2010), The palaeogeographic position of Central Iberia in Gondwana during the Ordovician: Evidence from zircon chronology and Nd isotopes, *Terra Nova*, 22, 341–346, doi:10.1111/j.1365-3121.2010.00957.x.
- Blanco, M. J., and W. Spakman (1993), The P wave velocity structure of the mantle below the Iberian Peninsula: Evidence for subducted lithosphere below southern Spain, *Tectonophysics*, 221, 13–34, doi:10.1016/0040-1951(93)90025-F.
- Bradley, D. C. (2011), Secular trends in the geologic record and the supercontinent cycle, *Earth Sci. Rev.*, 108, 16–33, doi:10.1016/j.earscirev.2011.05.003.
- Capdevila, R., and D. Mougenot (1988), Pre-Mesozoic basement of the Western Iberian continental margin and its place in the Variscan Belt, *Proc. Ocean Drill. Program Sci. Results*, 103, 3–12.
- Capdevila, R., M. Lamboy, and J. P. Lepêtre (1974), Découverte de granulites, de Charnockites et de syénites néphéliniques dans la partie occidentale de la marge continentale Nord espagnole, *C. R. Seances Acad. Sci., Ser. D*, 278, 17–20.
- Capote, R., J. A. Muñoz, J. L. Simón, C. L. Liesa, and L. E. Arlegui (2002), Alpine tectonics I: The Alpine system north of the Betic Cordillera, in *The Geology of Spain*, edited by W. Gibbons and T. Moreno, pp. 367–400, Geol. Soc., London.
- Carrapa, B. (2010), Resolving tectonic problems by dating detrital minerals, *Geology*, 38, 191–192, doi:10.1130/focus022010.1.
- Chantraine, J., E. Egal, D. Thiéblemont, E. Legoff, C. Guerrot, M. Ballèvre, and P. Guennoc (2001), The Cadomian active margin (North Armorican Massif, France): A segment of the North Atlantic Panafrican Belt, *Tectonophysics*, 331, 1–18, doi:10.1016/S0040-1951(00)00233-X.
- Chew, D. M., U. Schaltegger, J. Kosler, M. J. Whitehouse, M. Gutjahr, R. A. Spikings, and A. Miskovic (2007), U-Pb geochronologic evidence of the evolution of the Gondwanan margin of the north-central Andes, *Geol. Soc. Am. Bull.*, 119, 697–711, doi:10.1130/B26080.1.
- Choubert, G., and A. Faure-Muret (Eds.) (1990), *International Geological Map of Africa, 1:5,000,000*, 3rd ed., Comm. for the Geol. Map of the World, Bur. de Rech. Geol. et Min., UNESCO, Paris.
- Clauer, N., R. Caby, D. Jeannette, and R. Trompette (1982), Geochronology of sedimentary and metasedimentary Precambrian rocks of the West African craton, *Precambrian Res.*, 18, 53–71, doi:10.1016/0301-9268(82)90036-5.
- Cocks, L. R. M., and T. H. Torsvik (2002), Earth geography from 500 to 400 million years ago: A faunal and palaeomagnetic review, *J. Geol. Soc.*, 159, 631–644, doi:10.1144/0016-764901-118.
- Colchen, M. (1974), *Géologie de la Sierra de la Demanda (Burgos-Logroño, Espagne)*, *Mem. Inst. Geol. Min. Esp.*, vol. 85, 436 pp., Serv. de Publ., Minist. de Ind., Madrid.
- Condie, K. C., and R. C. Aster (2009), Zircon age episodicity and growth of continental crust, *Eos Trans. AGU*, 90(41), 364, doi:10.1029/2009EO410003.
- Condie, K. C., M. E. Bickford, R. C. Aster, E. Belousova, and D. W. Scholl (2011), Episodic zircon ages, Hf isotopic composition, and the preservation rate of continental crust, *Geol. Soc. Am. Bull.*, 123, 951–957, doi:10.1130/B30344.1.
- Cordani, U. G., and W. Teixeira (2007), Proterozoic accretionary belts in the Amazonian craton, in *4-D Framework of Continental Crust*, edited by R. D. Hatcher Jr. et al., *Mem. Geol. Soc. Am.*, 200, 297–320, doi:10.1130/2007.1200(14).
- Courjault-Radé, P., F. Debrenne, and A. Gandin (1992), Palaeogeographic and geodynamic evolution of the Gondwana continental margins during the Cambrian, *Terra Nova*, 4, 657–667, doi:10.1111/j.1365-3121.1992.tb00615.x.
- Cox, R., E. D. Gutman, and P. Hines (2002), Diagenetic origin for quartz-pebble conglomerates, *Geology*, 30, 323–326, doi:10.1130/0091-7613(2002)030<0323:DOFQPC>2.0.CO;2.
- Debrenne, F., and P. Courjault-Radé (1994), Répartition paléogéographique des archéocyathes et délimitation des zones intertropicales au Cambrien inférieur, *Bull. Soc. Geol. Fr.*, 165, 459–467.
- Diez Fernández, R., J. R. Martínez-Catalán, A. Gerdes, J. Abati, R. Arenas, and J. Fernández-Suárez (2010), U-Pb ages of detrital zircons from the basal allochthonous units of NW Iberia: Provenance and paleoposition on the northern margin of Gondwana during the Neoproterozoic and Paleozoic, *Gondwana Res.*, 18, 385–399, doi:10.1016/j.gr.2009.12.006.
- Eguíluz, L., J. I. Gil-Ibarra, B. Ábalos, and A. Apráiz (2000), Superposed Hercynian and Cadomian orogenic cycles in the Ossa-Morena zone and related areas of the Iberian Massif, *Mem. Geol. Soc. Am.*, 112, 1398–1413, doi:10.1130/0016-7606(2000)112<1398:SHACOC>2.0.CO;2.
- Evans, D. A. D., and R. N. Mitchell (2011), Assembly and breakup of the core of Paleoproterozoic-Mesoproterozoic supercontinent Nuna, *Geology*, 39, 443–446, doi:10.1130/G31654.1.
- Fernández-Suárez, J., G. Gutiérrez-Alonso, G. A. Jenner, and S. Jackson (1998), Geochronology and geochemistry of the Pola de Allande granitoids (northern Spain). Their bearing on the Cadomian/Avalonian evolution of NW Iberia, *Can. J. Earth Sci.*, 35, 1439–1453, doi:10.1139/e98-074.
- Fernández-Suárez, J., G. Gutiérrez-Alonso, G. A. Jenner, and M. N. Tubrett (2000), New ideas on the Proterozoic-Early Paleozoic evolution of NW Iberia: Insights from U-Pb detrital zircon ages, *Precambrian Res.*, 102, 185–206, doi:10.1016/S0301-9268(00)00065-6.
- Fernández-Suárez, J., G. Gutiérrez-Alonso, and T. E. Jeffries (2002), The importance of along-margin terrane transport in northern Gondwana: Insights from detrital zircon parentage in Neoproterozoic rocks from Iberia and Brittany, *Earth Planet. Sci. Lett.*, 204, 75–88, doi:10.1016/S0012-821X(02)00963-9.
- Fernández-Suárez, J., F. Díaz García, T. E. Jeffries, R. Arenas, and J. Abati (2003), Constraints on the provenance of the uppermost allochthonous terrane of the NW Iberian Massif: Inferences from detrital zircon U-Pb ages, *Terra Nova*, 15, 138–144, doi:10.1046/j.1365-3121.2003.00479.x.
- Fernández-Suárez, J., G. Gutiérrez-Alonso, S. T. Johnston, T. E. Jeffries, D. Pastor-Galán, G. A. Jenner, and J. B. Murphy (2011), Iberian late-Variscan granitoids: Some considerations on crustal sourced and the significance of “mantle extraction ages,” *Lithos*, 123, 121–132, doi:10.1016/j.lithos.2010.09.010.
- Garçon, M., C. Chauvel, and S. Bureau (2011), Beach placer, a proxy for the average Nd and Hf isotopic composition of a continental area, *Chem. Geol.*, 287, 182–192, doi:10.1016/j.chemgeo.2011.06.007.
- Gardien, V., N. Arnaud, and L. Desmurs (2000), Petrology and Ar-Ar dating of granulites from the Galicia Bank (Spain): African craton relics in Western Europe, *Geodin. Acta*, 13, 103–117, doi:10.1016/S0985-3111(00)00117-0.
- Garrido, C. J., and J.-L. Bodinier (1999), Diversity of mafic rocks in the Ronda peridotite: Evidence for pervasive melt/rock reaction during heating of subcontinental lithospheric mantle by upwelling asthenosphere, *J. Petrol.*, 40, 729–754, doi:10.1093/petrology/40.5.729.
- Guerrot, C., J. J. Peucat, R. Capdevila, and L. Dosso (1989), Archean protoliths within Early Proterozoic crust of the west European Hercynian belt: Possible relics of the west African craton, *Geology*, 17, 241–244, doi:10.1130/0091-7613(1989)017<0241:APWEPG>2.3.CO;2.
- Gutiérrez-Alonso, G., J. Fernández-Suárez, A. S. Collins, I. Abad, and F. Nieto (2005), Amazonian Mesoproterozoic basement in the core of the Ibero-Armorican Arc: 40Ar/39Ar detrital mica ages complement the zircons tale, *Geology*, 33, 637–640, doi:10.1130/G21485.1.
- Gutiérrez-Alonso, G., J. B. Murphy, J. Fernández Suárez, A. B. Weil, M. P. Franco, and J. C. Gonzalo (2011), Lithospheric delamination in the core of Pangea: Sm-Nd insights from the Iberian mantle, *Geology*, 39, 155–158, doi:10.1130/G31468.1.
- Gutiérrez-Marco, J. C., M. Robardet, I. Rábano, G. N. Sarmiento, M. A. San José Lancha, P. Herranz, and A. P. Pieren Pidal (2002), Ordovician, in *The Geology of Spain*, edited by W. Gibbons and T. Moreno, pp. 31–49, Geol. Soc., London.
- Hietpas, J., S. Samson, D. Moecher, and A. K. Schmitt (2010), Recovering tectonic events from the sedimentary record: Detrital monazite plays in high fidelity, *Geology*, 38, 167–170, doi:10.1130/G30265.1.
- Horton, B. K., J. E. Saylor, J. Nie, A. Mora, M. Parra, A. Reyes-Harker, and D. F. Stockli (2010), Linking sedimentation in the northern Andes to basement configuration, Mesozoic extension, and Cenozoic shortening: Evidence from detrital zircon U-Pb ages, Eastern Cordillera, Colombia, *Geol. Soc. Am. Bull.*, 122, 1423–1442, doi:10.1130/B30118.1.
- ILIHA DSS Group (1993), A deep seismic sounding investigation of lithospheric heterogeneity and anisotropy beneath the Iberian Peninsula, *Tectonophysics*, 221, 35–51.
- Jackson, S. E., N. J. Pearson, W. L. Griffin, and E. A. Belousova (2004), The application of laser ablation-inductively coupled plasma-mass spectrometry to in situ U-Pb zircon geochronology, *Chem. Geol.*, 211, 47–69, doi:10.1016/j.chemgeo.2004.06.017.
- Johnson, P. R., and B. Woldenhamnot (2003), Development of the Arabian-Nubian Shield: Perspectives on accretion and deformation in the northern East African Orogen and the assembly of Gondwana, in *Proterozoic East Gondwana: Supercontinental Assembly and Breakup*,

- edited by M. Yoshida, B. F. Windley, and S. Dasgupta, *Geol. Soc. Spec. Publ.*, 206, 289–325, doi:10.1144/GSL.SP.2003.206.01.15.
- Kröner, A., and R. J. Stern (2005), Pan-African Orogeny, in *Encyclopedia of Geology*, vol. 1, edited by R. C. Selley, L. R. M. Cocks, and I. R. Plimer, pp. 1–12, Elsevier, Amsterdam.
- Küster, D., J.-P. Liégeois, D. Matukov, S. Sergeev, and F. Lucassen (2008), Zircon geochronology and Sr, Nd, Pb isotope geochemistry of granitoids from Bayuda Desert and Sabaloka (Sudan): Evidence for a Bayudan event (920–900 Ma) preceding the Pan-African orogenic cycle (860–590 Ma) at the eastern boundary of the Saharan Metacraton, *Precambrian Res.*, 164, 16–39, doi:10.1016/j.precamres.2008.03.003.
- Lawrence, R. L., R. Cox, R. W. Mapes, and D. S. Coleman (2010), Hydrodynamic fractionation of zircon age populations, *Geol. Soc. Am. Bull.*, 123, 295–305, doi:10.1130/B30151.1.
- Liñán, E., A. Perejón, and K. Szalay (1993), The Lower-Middle Cambrian stages and stratotypes from the Iberian Peninsula: A revision, *Geol. Mag.*, 130, 817–833, doi:10.1017/S0016756800023189.
- Liñán, E., R. Gozalo, T. Palacios, J. A. Gámez-Vintaned, J. M. Ugidos, and E. Mayoral (2002), Cambrian, in *The Geology of Spain*, edited by W. Gibbons and T. Moreno, pp. 17–29, Geol. Soc., London.
- Liñán, E., M. E. Dies, J. A. Gámez-Vintaned, R. Gozalo, E. Mayoral, and F. Muñoz (2005), Lower Ovetian (Lower Cambrian) trilobites and biostratigraphy of the Pedroche Formation (Sierra de Córdoba, southern Spain), *Geobios*, 38, 365–381, doi:10.1016/j.geobios.2003.11.007.
- Linnemann, U., M. F. Pereira, T. E. Jeffries, K. Drost, and A. Gerdes (2008), The Cadomian Orogeny and the opening of the Rheic Ocean: The diachronous geotectonic processes constrained by LA-ICP-MS U-Pb zircon dating (Ossa-Morena and Saxo-Thuringian Zones, Iberian and Bohemian Massifs), *Tectonophysics*, 461, 21–43, doi:10.1016/j.tecto.2008.05.002.
- Linnemann, U., K. Ouzegane, A. Drareni, M. Hofmann, S. Becker, A. Gärtner, and A. Sagawe (2011), Sands of West Gondwana: An archive of secular magmatism and plate interactions—a case study from the Cambro-Ordovician section of the Tassili Ouan Ahaggar (Algerian Sahara) using U-Pb-LA-ICP-MS detrital zircon ages, *Lithos*, 123, 188–203, doi:10.1016/j.lithos.2011.01.010.
- Ludwig, K. R. (2001), *Isoplot v. 2.2: A geochronological toolkit for Microsoft Excel. Spec. Publ. 1a*, 53 pp., Berkeley Geochronol. Cent., Berkeley, Calif.
- Mac Niocaill, C., B. A. Van der Pluijm, R. Van Der Voo, and A. K. McNamara (2002), Discussion and Reply: West African proximity of the Avalon terrane in the latest Precambrian, *Geol. Soc. Am. Bull.*, 114, 1051–1052, doi:10.1130/0016-7606(2002)114<1051:R>2.0.CO;2.
- Maloof, A. C., S. M. Porter, J. L. Moore, F. Ó. Dudás, S. A. Bowring, J. A. Higgins, D. A. Fike, and M. P. Eddy (2010a), The earliest Cambrian record of animals and ocean geochemical change, *Geol. Soc. Am. Bull.*, 122, 1731–1774, doi:10.1130/B30346.1.
- Maloof, A. C., J. Ramezani, S. A. Bowring, D. A. Fike, S. M. Porter, and M. Mazouad (2010b), Constraints on early Cambrian carbon cycling from the duration of the Nemakit-Daldynian-Tommotian boundary $\delta^{13}\text{C}$ shift, Morocco, *Geology*, 38, 623–626, doi:10.1130/G30726.1.
- Mapes, R. W., D. S. Coleman, A. Nogueira, and T. Housh (2004), How far do zircons travel? Evaluating the significance of detrital zircon provenance using the modern Amazon River fluvial system, *Geol. Soc. Am. Abstr. Programs*, 36(7), 78.
- Matte, P. (1991), Accretionary history and crustal evolution of the Variscan belt in Western Europe, *Tectonophysics*, 196, 309–337, doi:10.1016/0040-1951(91)90328-P.
- McCausland, P. J. A., J. B. Murphy, and C. MacNiocaill (2006), Endings and beginnings: Paleogeography of the Neoproterozoic-Cambrian transition, *Precambrian Res.*, 147, 187–192, doi:10.1016/j.precamres.2006.01.014.
- Michard, A., A. Soulaïmani, C. Hoepffner, H. Ouanaimi, L. Baïdder, E. C. Rjimat, and O. Saddiqi (2010), The south-western branch of the Variscan belt: Evidence from Morocco, *Tectonophysics*, 492, 1–24, doi:10.1016/j.tecto.2010.05.021.
- Morag, N., D. Avigad, A. Gerdes, E. Belousova, and Y. Harlavan (2011a), Crustal evolution and recycling in the northern Arabian-Nubian Shield: New perspectives from zircon Lu-Hf and U-Pb systematics, *Precambrian Res.*, 186, 101–116, doi:10.1016/j.precamres.2011.01.004.
- Morag, N., D. Avigad, A. Gerdes, E. Belousova, and Y. Harlavan (2011b), Detrital zircon Hf isotopic composition indicates long distance transport of North Gondwana Cambrian-Ordovician sandstones, *Geology*, 39, 955–958, doi:10.1130/G32184.1.
- Müller, W., M. Shelley, P. Miller, and S. Broude (2009), Initial performance metrics of a new custom-designed ArF excimer LA-ICPMS system coupled to a two-volume laser-ablation cell, *J. Anal. At. Spectrom.*, 24, 209–214, doi:10.1039/b805995sk.
- Murphy, J. B., and G. Gutiérrez-Alonso (2008), The origin of the Variscan upper allochthons in the Ordeal Complex, northwestern Iberia: Sm-Nd isotope constraints on the closure of the Rheic Ocean, *Can. J. Earth Sci.*, 45, 651–668, doi:10.1139/E08-019.
- Murphy, J. B., R. D. Nance, and J. D. Keppie (2002), Discussion and Reply: West African proximity of the Avalon terrane in the latest Precambrian, *Geol. Soc. Am. Bull.*, 114, 1049–1050, doi:10.1130/0016-7606(2002)114<1049:DARWAP>2.0.CO;2.
- Murphy, J. B., S. A. Pisarevsky, R. D. Nance, and J. D. Keppie (2004), Neoproterozoic—Early Paleozoic evolution of peri-Gondwanan terranes: Implications for Laurentia-Gondwana connections, *Int. J. Earth Sci.*, 93, 659–682, doi:10.1007/s00531-004-0412-9.
- Murphy, J. B., G. Gutiérrez-Alonso, R. D. Nance, J. Fernández-Suárez, J. D. Keppie, C. Quesada, R. A. Strachan, and J. Dostal (2006), Origin of the Rheic Ocean: Rifting along a Neoproterozoic suture?, *Geology*, 34, 325–328, doi:10.1130/G22068.1.
- Murphy, J. B., G. Gutiérrez-Alonso, J. Fernández-Suárez, and J. A. Braid (2008), Probing crustal and mantle lithosphere origin through Ordovician volcanic rocks along the Iberian passive margin of Gondwana, *Tectonophysics*, 461, 166–180, doi:10.1016/j.tecto.2008.03.013.
- Murphy, J. B., R. D. Nance, G. Gutiérrez-Alonso, and J. D. Keppie (2009), Supercontinent reconstruction from recognition of leading continental edges, *Geology*, 37, 595–598, doi:10.1130/G25725A.1.
- Nägler, T. F. (1990), Sm-Nd, Rb-Sr and common lead isotope geochemistry on fine-grained sediments of the Iberian Massif, PhD thesis, 141 pp., ETH Zurich, Zurich, Switzerland.
- Nägler, T. F., H. J. Schäfer, and D. Gebauer (1992), A Sm-Nd isochron on pelites 1 Ga in excess of their depositional age and its possible significance, *Geochim. Cosmochim. Acta*, 56, 789–795, doi:10.1016/0016-7037(92)90098-4.
- Nägler, T. F., H. J. Schäfer, and D. Gebauer (1995), Evolution of the Western European continental crust: Implications from Nd and Pb isotopes in Iberian sediments, *Chem. Geol.*, 121, 345–357, doi:10.1016/0009-2541(94)00129-V.
- Nance, R. D., J. B. Murphy, R. A. Strachan, J. D. Keppie, G. Gutiérrez-Alonso, J. Fernández-Suárez, C. Quesada, U. Linnemann, R. D’Lemos, and S. A. Pisarevsky (2008), Neoproterozoic-early Palaeozoic tectonostratigraphy and palaeogeography of the peri-Gondwanan terranes: Amazonia vs. West African connections, in *The Boundaries of the West African Craton*, edited by N. Ennih and J.-P. Liégeois, *Geol. Soc. Spec. Publ.*, 297, 345–383.
- Paquette, J. L., and M. Tiepolo (2007), High resolution (5 μm) U-Th-Pb isotope dating of monazite with excimer laser ablation (ELA)-ICPMS, *Chem. Geol.*, 240, 222–237, doi:10.1016/j.chemgeo.2007.02.014.
- Peng, S., and L. Babcock (2008), Cambrian Period, in *The Concise Geological Time Scale*, edited by J. G. Ogg, G. Ogg, and F. M. Gradstein, pp. 37–46, Cambridge Univ. Press, Cambridge, U. K.
- Pin, C., J. L. Paquette, B. Ábalos, F. J. Santos, and J. I. Gil Ibarra (2006), Composite origin of an early Variscan transported suture: Ophiolitic units of the Morais Nappe Complex (north Portugal), *Tectonics*, 25, TC5001, doi:10.1029/2006TC001971.
- Prokopyev, A. V., J. Toro, E. L. Miller, and G. E. Gehrels (2008), The paleo-Lena River—200 m.y. of transcontinental zircon transport in Siberia, *Geology*, 36, 699–702, doi:10.1130/G24924A.1.
- Quesada, C. (1990), Precambrian terranes in the Iberian Variscan Foldbelt, in *Avalonian and Cadomian Geology of the North Atlantic*, edited by R. A. Strachan and G. K. Taylor, pp. 109–133, Blackie, Glasgow, U. K.
- Quesada, C., F. Bellido, R. D. Dallmeyer, I. Gil-Ibarra, J. T. Oliveira, A. Pérez-Estaun, A. Ribeiro, M. Robardet, and J. B. Silva (1991), Terranes within the Iberian Massif: Correlations with West African sequences, in *The West African Orogens and Circum-Atlantic Correlatives*, edited by R. D. Dallmeyer and J. P. Lécroché, pp. 267–293, Springer, Berlin.
- Ramírez-Merino, J. I., A. Olivé-Davó, M. Álvaro-López, and A. Hernández-Samaniego (1990), Mapa y Memoria de la Hoja n° 241 (Anguiano) del Mapa Geológico de España a escala 1:50.000 (Serie MAGNA), Inst. Geol. y Min. de Esp., Madrid.
- Robb, L. J., A. H. Knoll, K. A. Plumb, G. A. Shields, H. Strauss, and J. Veizer (2004), The Precambrian: The Archean and Proterozoic cons, in *A Geological Time Scale 2004*, edited by F. M. Gradstein, J. G. Ogg, and A. G. Smith, pp. 129–140, Cambridge Univ. Press, Cambridge, U. K.
- Rooney, A. D., D. Selby, J.-P. Houzay, and P. R. Renne (2010), Re-Os geochronology of a Mesoproterozoic sedimentary succession, Taoudeni basin, Mauritania: Implications for basin-wide correlations and Re-Os organic-rich sediment systematics, *Earth Planet. Sci. Lett.*, 289, 486–496, doi:10.1016/j.epsl.2009.11.039.
- Rubio-Ordóñez, A. (2010), Magmatismo Neoproterozoico en el Antiforme del Narcea, PhD thesis, 306 pp., Univ. de Oviedo, Asturias, Spain.

- Sánchez-Martínez, S., T. Jeffries, R. Arenas, J. Fernández-Suárez, and R. García-Sánchez (2006), A pre-Rodinian ophiolite involved in the Variscan suture of Galicia (Cabo Ortegal Complex, NW Spain), *J. Geol. Soc.*, *163*, 737–740, doi:10.1144/0016-76492006-030.
- Sánchez-Martínez, S., R. Arenas, A. Gerdes, P. Castiñeiras, A. Potrel, and J. Fernández Suárez (2011), Isotope geochemistry and revised geochronology of the Purrido Ophiolite (Cabo Ortegal Complex, NW Iberian Massif): Devonian magmatism with mixed sources and involved Mesoproterozoic basement, *J. Geol. Soc.*, *168*, 733–750, doi:10.1144/0016-76492010-065.
- Santos, J. F., U. Schärer, J. I. Gil-Ibarguchi, and J. Girardeau (2002), Genesis of pyroxenite-rich peridotite at Cabo Ortegal (NW Spain): Geochemical and Pb-Sr-Nd isotope data, *J. Petrol.*, *43*, 17–43, doi:10.1093/ptology/43.1.17.
- Schobbenhaus, C., and A. Bellizia (Eds.) (2001), *Geological Map of South America, 1:5,000,000*, Comm. for the Geol. Map of the World, UNESCO, Brasilia.
- Scholl, D. W., and R. Von Huene (2007), Crustal recycling at modern subduction zones applied to the past—Issues of growth and preservation of continental basement crust, mantle geochemistry, and supercontinent reconstruction, in *4-D Framework of Continental Crust*, edited by R. D. Hatcher Jr. et al., *Mem. Geol. Soc. Am.*, *200*, 9–32, doi:10.1130/2007.1200(02).
- Shergold, J. H., and R. H. Cooper (2004), The Cambrian Period, in *A Geological Time Scale 2004*, edited by F. M. Gradstein, J. G. Ogg, and A. G. Smith, pp. 147–164, Cambridge Univ. Press, Cambridge, U. K.
- Shergold, J. H., E. Liñán, and T. Palacios (1983), Late Cambrian trilobites from the Najerilla Formation, north-eastern Spain, *Palaeontology*, *26*, 71–92.
- Souriau, A., S. Chevrot, and C. Olivera (2008), A new tomographic image of the Pyrenean lithosphere from teleseismic data, *Tectonophysics*, *460*, 206–214, doi:10.1016/j.tecto.2008.08.014.
- Tera, F., and G. J. Wasserburg (1973), A response to a comment on U-Pb systematics in lunar basalts, *Earth Planet. Sci. Lett.*, *19*, 213–217, doi:10.1016/0012-821X(73)90117-9.
- Thomas, R. J., A. Fekkak, N. Ennih, E. Errami, S. C. Loughlin, P. G. Gresse, L. P. Chevalier, and J. P. Liégeois (2004), A new lithostratigraphic framework for the Anti-Atlas Orogen, Morocco, *J. Afr. Earth Sci.*, *39*, 217–226, doi:10.1016/j.jafrearsci.2004.07.046.
- Thompson, M. D., A. M. Grunow, and J. Ramezani (2007), Late Neoproterozoic paleogeography of the Southeastern New England Avalon Zone: Insights from U-Pb geochronology and paleomagnetism, *Geol. Soc. Am. Bull.*, *119*, 681–696, doi:10.1130/B26014.1.
- Tiepolo, M. (2003), In situ Pb geochronology of zircon with laser ablation-inductively coupled plasma-sector field mass spectrometry, *Chem. Geol.*, *141*, 1–19.
- Tohver, E., M. S. D'Agrella-Filho, and R. I. F. Trindale (2006), Paleomagnetic record of Africa and South America for the 1200–500 Ma interval, and evaluation of Gondwana and Rodinia assemblies, *Precambrian Res.*, *147*, 193–222, doi:10.1016/j.precamres.2006.01.015.
- Tubía, J. M., J. Cuevas, and J. J. Esteban (2004), Tectonic evidence in the Ronda peridotites, Spain, for mantle diapirism related to delamination, *Geology*, *32*, 941–944, doi:10.1130/G20869.1.
- Ugidos, J. M., I. Armenteros, P. Barba, M. I. Valladares, and J. R. Colmenero (1997), Geochemistry and petrology of recycled orogen-derived sediments: A case study from Upper Precambrian siliciclastic rocks of the Central Iberian Zone, Iberian Massif, Spain, *Precambrian Res.*, *84*, 163–180, doi:10.1016/S0301-9268(97)00023-5.
- Ugidos, J. M., J. M. Sánchez-Santos, P. Barba, and M. I. Valladares (2010), Upper Neoproterozoic series in the Central Iberian, Cantabrian and West Asturian Leonese Zones (Spain): Geochemical data and statistical results as evidence for a shared homogenised source area, *Precambrian Res.*, *178*, 51–58, doi:10.1016/j.precamres.2010.01.009.
- Unrug, R. (Ed.) (1996), Geodynamic map of Gondwana supercontinent assembly, 4 sheets, scale 1:10,000,000, Ed. du Bureau de Rech. Geol. et Min., Orléans, France.
- Unrug, R. (1997), Rodinia to Gondwana: The geodynamic map of Gondwana supercontinent assembly, *GSA Today*, *7*, 1–6.
- Valladares, M. I., P. Barba, and J. M. Ugidos (2002a), Precambrian, in *The Geology of Spain*, edited by W. Gibbons and T. Moreno, pp. 7–16, Geol. Soc., London.
- Valladares, M. I., J. M. Ugidos, P. Barba, and J. R. Colmenero (2002b), Contrasting geochemical features of the Central Iberian Zone shales (Iberian Massif, Spain): Implications for the evolution of Neoproterozoic-lower Cambrian sediments and their sources in other peri-Gondwanan areas, *Tectonophysics*, *352*, 121–132, doi:10.1016/S0040-1951(02)00192-0.
- van Acherbergh, E., C. G. Ryan, S. E. Jackson, and W. Griffin (2001), Data reduction software for LA-ICP-MS, in *Laser Ablation ICPMS in the Earth Sciences: Principles and Applications*, edited by P. Sylvester, *Short Course Ser. Mineral. Assoc. Can.*, *29*, 239–243.
- Van der Wal, D., and J. L. Bodinier (1996), Origin of the recrystallisation front in the Ronda peridotite by km-scale pervasive porous melt flow, *Contrib. Mineral. Petrol.*, *122*, 387–405, doi:10.1007/s004100050135.
- Vauchez, A., and G. Barruol (1996), Shear-wave splitting in the Appalachians and the Pyrenees: Importance of the inherited tectonic fabric of the lithosphere, *Phys. Earth Planet. Inter.*, *95*, 127–138, doi:10.1016/0031-9201(95)03125-1.
- Vauchez, A., and C. J. Garrido (2001), Seismic properties of an asthenospherized lithospheric mantle: Constraints from lattice preferred orientations in peridotite from the Ronda massif, *Earth Planet. Sci. Lett.*, *192*, 235–249, doi:10.1016/S0012-821X(01)00448-4.
- Vauchez, A., and A. Nicolas (1991), Mountain building: Strike-parallel motion and mantle anisotropy, *Tectonophysics*, *185*, 183–201, doi:10.1016/0040-1951(91)90443-V.
- Vauchez, A., G. Barruol, and A. Tommasi (1997), Why do continents break-up parallel to ancient orogenic belts?, *Terra Nova*, *9*, 62–66, doi:10.1111/j.1365-3121.1997.tb00003.x.
- Vidal, G., T. Palacios, J. A. Gámez-Vintaned, M. A. Díez-Balda, and S. W. F. Grant (1994), Neoproterozoic-early Cambrian geology and palaeontology of Iberia, *Geol. Mag.*, *131*, 729–765, doi:10.1017/S001675680001284X.
- Villaseca, C., E. Belousova, D. Orejana, P. Castiñeiras, and C. Pérez-Soba (2011), Presence of Palaeoproterozoic and Archean components in the granulite-facies rocks of central Iberia: The Hf isotopic evidence, *Precambrian Res.*, *187*, 143–154, doi:10.1016/j.precamres.2011.03.001.
- Weil, A. B., R. Van Der Voo, C. Mac Niocaill, and J. G. Meert (1998), The Proterozoic supercontinent Rodinia: Paleomagnetically derived reconstructions for 1100–800 Ma, *Earth Planet. Sci. Lett.*, *154*, 13–24, doi:10.1016/S0012-821X(97)00127-1.
- Wiedenbeck, M., P. Allé, F. Corfu, W. L. Griffin, M. Meier, F. Oberli, A. von Quadt, J. C. Roddick, and W. Spiegel (1995), Three natural zircon standards for U-Th-Pb, Lu-Hf, trace element and REE analyses, *Geostand. Geoanal. Res.*, *19*(1), 1–23, doi:10.1111/j.1751-908X.1995.tb00147.x.
- Zeck, H. P., M. T. D. Wingate, G. D. Pooley, and J. M. Ugidos (2004), A sequence of Pan-African and Hercynian events recorded in zircons from an orthogneiss from the Hercynian belt of western Central Iberia—an ion microprobe study, *J. Petrol.*, *45*, 1613–1629, doi:10.1093/ptology/egh026.